purified 5' RACE PCR product was cloned into a plasmid (pBluescript SKII+) and then amplified in *E. coli*. Several clones were sequenced from both directions using a DNA sequencer.

*Immunoblot analysis:* Protein samples were obtained by dissolving cells in lysis buffer consisting of 1% sodium dodecyl sulfate (SDS), 10 mM Tris-HCl (pH 6.8), 10% glycerol, 1 mM EDTA, and 10 µL/mL protease inhibitor cocktail (Sigma, St. Louis, MO). Protein samples were boiled for 10 min and centrifuged at 8,000x g for 10 min at 4 °C. Supernatants were separated and used as a whole cell extract. The proteins (100 µg) were electrophoresed on an SDS-polyacrylamide gel and subsequently electrotransferred to a poly vinylidene difluoride membrane. The membranes were incubated with goat polyclonal anti-human M-cadherin antibody (1:500; Santa Cruz Biotechnology, Santa Cruz, CA) for 16 h at 4 °C as the primary antibody using blocking agent solution (Block Ace; Dainihon Pharmaceutical Co., Osaka, Japan). There was apparently sufficient antibody cross-reactivity between human and rat M-cadherin. The membranes were subsequently incubated with horseradish peroxidase conjugated anti-goat IgG as the secondary antibody. The bands were visualized with an enhanced chemiluminescence kit (Amersham, Buckinghamshire, UK).

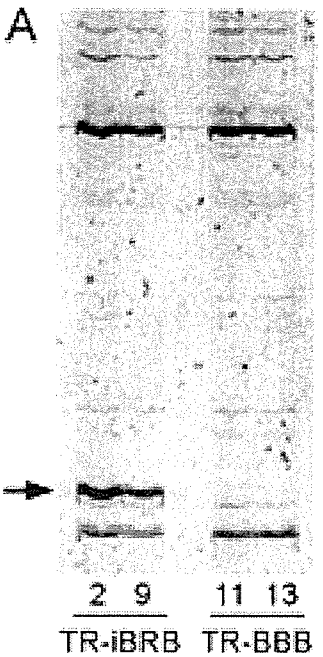


## RESULTS

The differential display analysis of TR-iBRB2, TR-iBRB9, TR-BBB11, and TR-BBB13 cells showed 40 bands, which were selectively expressed more in TR-iBRB cells than in the TR-iBBB cells (Figure 1A). These DNA bands of 100 to about 450 bp were cloned and sequenced. Quantitative real time PCR using specific primers for each clone was performed to confirm the reproducibility. As a result of these analyses, eight clones were identified and found to be expressed to a greater extent in TR-iBRB cells than in TR-BBB cells (Table 1). The differential displayed clones included two sequences homologous to mouse genes, such as M-cadherin (cadherin-15; clone 1), GATA-binding protein 3 (GATA-3; clone 2), and one sequence identical to rat cytosolic branched chain amino transferase (BCATc; clone 4). The other five sequences (clones 3, 5, 6, 7, and 8) were only found in the expressed sequence tag (EST) or genomic sequences.

Clone 1, of 251 bp, which was expressed 213 fold more intensely in TR-iBRB cells than in TR-BBB cells, exhibited

**B**:

```
Clone 1              1 TTTTTGGCTCCATGGCAGATAAACTCACTGAAGGTCATCTGTGTGAGCTCC    51
Mouse M-cadherin  3080 ---------------------------------------------------  3080

Clone 1             52 AGGGGAGGACTGAGTCCTGTATGGGCTAGGCAGCG-GAGGGAGAGCGCTCT   101
Mouse M-cadherin  3080 --------------------ATGGACTAGGCAGCTAGAGGGAGCACTGTCC  3110
                                           **** *********  *******  *  **

Clone 1            102 CCCTCTGGAGTGCAGAAGCCACC-TTCAATCACCCTGCTAGGGTTCATCCC   151
Mouse M-cadherin  3111 TGGCA--GAGTGCAGAAGCCACCCTTAGTG--CCCTGCTAGGGCTCATCCC  3157
                       ***************** **      *********** *******

Clone 1            152 ATCTTTGTGTCCCAGTTGTGACTCTCACCTCTGTATGAAA-GCAGGCATCT   201
Mouse M-cadherin  3158 ATCTTTGATTCCCAGTTGTGACTCTTGCCTCTGTATGAAAAGCAGGCGTCT  3208
                       *******  ****************  ************* ****** ***

Clone 1            202 AAGGAGCAGATTGGAATTAAAAACA-ACTGTTCAGTGAAAAAAAAAAAAAA   251
Mouse M-cadherin  3209 AAAGAGTGGATTTCAATTAAAAGCATACTATTTGGGGGATCCAAAAAAAA   3258
                       ** ***  ****  ******** ** *** **  * * *   ********
```

Figure 1. Differential display analysis of TR-iBRB and TR-BBB cells. **A**: Typical fluorescent image of polyacrylamide gel electrophoresis. An arrow indicates selectively expressed DNA bands in TR-iBRB cells. DNA bands were cloned and sequenced. **B**: Nucleotide sequence of the selectively expressed clone (clone 1) marked by the arrow in **A**. Clone 1 sequence after nucleotide position 72 has 77% nucleotide homology with the 3' terminal of the mouse M-cadherin gene.

the largest difference in mRNA expression level of the eight clones. The sequence of clone 1 following nucleotide position 72 exhibited 77% nucleotide identity to the 3' terminal of the mouse M-cadherin gene (Figure 1B) [12]. By performing 5' RACE, a 2686 bp cDNA fragment was amplified as a rat M-cadherin. This sequence includes the clone 1 sequence and an open reading frame of 2355 nucleotides, which corresponds to 784 amino acid residues (Figure 2). The deduced amino acid sequence exhibits 97% and 86% identity to mouse and human M-cadherin, respectively [12,13], suggesting that the amplified DNA fragment represents the rat homolog of the M-cadherin gene.

```
   1  TCCCGCCGCTGCCCCCATGAGTTCTGCTCTGCTCTTCGCCCTCGGGCTGCTTGCCCAGAGCCTTGGCCTCTCCTGGGCAGTCCCTGAGCCTGAACCCAGCACCCTGTACCCCTGGCGCCGGGCA  124
   1                  M  S  S  A  L  L  F  A  L  G  L  L  A  Q  S  L  G  L  S  W  A  V  P  E  P  E  P  S  T  L  Y  P  W  R  R  A   36

 125  TCAGCCCCAGGCCGTGTGCGGAGAGCCTGGGTCATCCCACCCATCAGTGTGTCTGAGAACCACAAACGCCTCCCCTACCCACTTGTGCAGATCAAGTCTGACAAACAACAGCTAGGCAGTGTC  247
  37  S  A  P  G  R  V  R  R  A  W  V  I  P  P  I  S  V  S  E  N  H  K  R  L  P  Y  P  L  V  Q  I  K  S  D  K  Q  Q  L  G  S  V   77
                                 ^ EC1->

 248  ATCTACAGTATCCAGGGTCCCGGTGTGGACGAGGAGCCCCGAAACGTCTTCTCCATCGACAAGTTCACTGGGAGGGTGTACCTCAATGCCACTCTGGACCGTGAGAAGACGGACCGCTTCAGG  370
  78  I  Y  S  I  Q  G  P  G  V  D  E  E  P  R  N  V  F  S  I  D  K  F  T  G  R  V  Y  L  N  A  T  L  D  R  E  K  T  D  R  F  R  118

 371  CTGAGGGCCTTTGCCCTGGACTTGGGTGGCTCTACCCTGGAGGACCCCACGGACCTGGAGATCGTCGTGGTGGATCAAAATGACAACCGGCCAGTCTTCCTACAGGATGTGTTCAGAGGCCGC  493
 119  L  R  A  F  A  L  D  L  G  G  S  T  L  E  D  P  T  D  L  E  I  V  V  V  D  Q  N  D  N  R  P  V  F  L  Q  D  V  F  R  G  R  159
                                                                                                                  EC2->

 494  ATCCTGGAGGGTGCCATCCCAGGCACCTTCGTAACCAGGGCTGAGGCCACAGATGCCGACGATCCGGAGACAGACAATGCGGCCCTCAGGTTCTCTATCCTGGAGCAGGGCAGCCCTGAGTTG  616
 160  I  L  E  G  A  I  P  G  T  F  V  T  R  A  E  A  T  D  A  D  D  P  E  T  D  N  A  A  L  R  F  S  I  L  E  Q  G  S  P  E  L  200

 617  TTCAGCATTGACGAGCACACTGGAGAGATCCGCACAGTGCAAGTGGGGCTGGACCGTGAGGTGGTGGCTGTGTACAACCTGACCTTGCAGGTGGCAGACATGTCCGGAGATGGCCTCACCGCC  739
 201  F  S  I  D  E  H  T  G  E  I  R  T  V  Q  V  G  L  D  R  E  V  V  A  V  Y  N  L  T  L  Q  V  A  D  M  S  G  D  G  L  T  A  241

 740  ACAGCCTCGGCCATCATCTCCGTAGATGACGTCAACGACAATGCCCCCGAGTTCACCAAGGATGAGTTCTTTATGGAGGCTGCAGAGGCTGTCAGTGGAGTGGACGTGGGACGGCTTGAGGTA  862
 242  T  A  S  A  I  I  S  V  D  D  V  N  D  N  A  P  E  F  T  K  D  E  F  F  M  E  A  A  E  A  V  S  G  V  D  V  G  R  L  E  V  282
                                                                EC3->

 863  GAAGACAAGGATCTGCCCGGTTCCCCCAACTGGGTGGCCAGGTTCACCATCCTGGAAGGCGATCCTGACGGGCAGTTCAAGATCTATACGGACCCCAAGACCAATGAAGGTGTGCTGTCCGTG  985
 283  E  D  K  D  L  P  G  S  P  N  W  V  A  R  F  T  I  L  E  G  D  P  D  G  Q  F  K  I  Y  T  D  P  K  T  N  E  G  V  L  S  V  323

 984  GTCAAGCCCCTGGATTATGAGAGCCGTGAGCAGTATGAGCTCAGAGTGTCTGTACAGAACGAGGCCCCTCTGCAGACAGCTGCCCCCCGGGCCCAGCGGGGCCAGACCAGGGTCAGTGTGTGG 1108
 324  V  K  P  L  D  Y  E  S  R  E  Q  Y  E  L  R  V  S  V  Q  N  E  A  P  L  Q  T  A  A  P  R  A  Q  R  G  Q  T  R  V  S  V  W  364

1109  GTTCAGGACACCAACGAGGCTCCAGTGTTTCCAGAGAACCCACTGAGGACGAGCATAGCTGAAGGAGCCCCGCCAGGCACCTCTGTGGCCACCTTCTCTGCCCGAGACCCTGACACGGAACAG 1231
 365  V  Q  D  T  N  E  A  P  V  F  P  E  N  P  L  R  T  S  I  A  E  G  A  P  P  G  T  S  V  A  T  F  S  A  R  D  P  D  T  E  Q  405
                                  EC4->

1232  CTGCAGAGAATCAGCTACTCTAAGGACTACGACCCAGAAGACTGGCTGCAAGTGGACCGGGCCACAGGCAGGATTCAGACCCAGCGAGTGTTGAGCCCTGCCTCACCCTTTTTAAAGGACGGC 1354
 406  L  Q  R  I  S  Y  S  K  D  Y  D  P  E  D  W  L  Q  V  D  R  A  T  G  R  I  Q  T  Q  R  V  L  S  P  A  S  P  F  L  K  D  G  446

1355  TGGTACAGGGCCATCATCCTAGCCCTGGACAACGCCATGCCTCCCAGCACAGCCACAGGCACCCTGTCCATTGAGATCTTAGAAGTCAACGACCATGCCCCTGCACTGGCCCCTCCTCTGTCT 1477
 447  W  Y  R  A  I  I  L  A  L  D  N  A  M  P  P  S  T  A  T  G  T  L  S  I  E  I  L  E  V  N  D  H  A  P  A  L  A  P  P  L  S  487
                                                                                                                  EC5->

1478  GGCAGCTTGTGCAGTGAACCGGACCAAGGCCCCGGTCTCCTCTTGGGTGCCACGGATGAGGACCTGCCCCCGCACGGGGCCCCCTTCCACTTCCAGCTGAACCCCAGGGTACCAGATCTCGGC 1600
 488  G  S  L  C  S  E  P  D  Q  G  P  G  L  L  L  G  A  T  D  E  D  L  P  P  H  G  A  P  F  H  F  Q  L  N  P  R  V  P  D  L  G  528

1601  CGGAACTGGAGCCTCAGCCAGATTAACGTGAGCCATGCACGCTTGCGGCTCCGACACCAGGTCTCTGAGGGCCTGCATCGCCTGAGCCTGCTGCTCCAGGACTCTGGGGAGCCGCCCCAGCAG 1723
 529  R  N  W  S  L  S  Q  I  N  V  S  H  A  R  L  R  L  R  H  Q  V  S  E  G  L  H  R  L  S  L  L  L  Q  D  S  G  E  P  P  Q  Q  569

1724  CGAGAGCAAACGCTGAACGTTACCGTGTGTCGCTGTGGGTTGGATGGCACCTGCCTGCCCGGGGCCGCTGCGCTGCAAGGAGGAGGTGTAGGCGTCGGCTTGGGCGCACTGGTCATTGTGCTG 1846
 570  R  E  Q  T  L  N  V  T  V  C  R  C  G  L  D  G  T  C  L  P  G  A  A  A  L  Q  G  G  G  V  G  V  G  L  G  A  L  V  I  V  L  610

1847  GCCAGCACCGTGGTCCTACTGGTTCTCATCCTGCTTGCTGCGCTCCGCACACGGTTCCGGGGGCAGTCTCGGAGCAAGAGTCTGTTGCATGGGCTTCAGGAGGATCTTCGGGACAACATTCTT 1969
 611  A  S  T  V  V  L  L  V  L  I  L  L  A  A  L  R  T  R  F  R  G  Q  S  R  S  K  S  L  L  H  G  L  Q  E  D  L  R  D  N  I  L  651

1970  AACTACGATGAACAAGGAGGCGGGGAGGAGGACCAGGATGCCTACGACATAAACCAGCTGCGCCACCCAGTGGAACCGAAGGCCACCAGCCGCTCTTTGGGCCGGCCACCCCTGCGCAGGGAT 2092
 652  N  Y  D  E  Q  G  G  G  E  E  D  Q  D  A  Y  D  I  N  Q  L  R  H  P  V  E  P  K  A  T  S  R  S  L  G  R  P  P  L  R  R  D  692

2093  GCACCCTTCAGCTATGTGCCACAGCCACATCGAGTACTTCCTACCAGCCCGTCTGACATCGCCAACTTCATCAGTGACGGCTTGGAGGCTGCGGACAGCGACCCCAGCGTGCCTCCCTATGAC 2215
 693  A  P  F  S  Y  V  P  Q  P  H  R  V  L  P  T  S  P  S  D  I  A  N  F  I  S  D  G  L  E  A  A  D  S  D  P  S  V  P  P  Y  D  733

2216  ACAGCTCTCATCTATGACTACGAGGGAGATGGCTCTGTGGCAGGGACCCTGAGCTCCATCCTGTCCAGCCAGGGAGATGAAGACCAGGACTATGACTATCTCCGGGACTGGGGCCCCCGCTTT 2338
 734  T  A  L  I  Y  D  Y  E  G  D  G  S  V  A  G  T  L  S  S  I  L  S  S  Q  G  D  E  D  Q  D  Y  D  Y  L  R  D  W  G  P  R  F  774

2339  GCTCGGCTGGCGGACATGTATGGGCATCCGTGAGAGCCAGAGCCAGGGGCAGACGTCCTGTGTGGACACGCCCACTCGGCCCAAACAAGGAGGCTCTCTCCTGGGACATGCACCCAGAAATCC 2461
 775  A  R  L  A  D  M  Y  G  H  P  *                                                                                              784

2462  TATGAGGGTCAGCAGCACGACCCATCTTTGGCTCCATGGCAGATAAACTCACTGAAGGTCATCTGTGTGAGCTCCAGGGGAGGACTGAGTCCTGTATGGGCTAGGCAGCGGAGGGAGAGCGCT 2584
2585  CTCCCTCTGGAGTGCAGAAGCCACCTTCAATCACCCTGCTAGGGTTCATCCCATCTTTGTGTCCCAGTTGTGACTCTCACCTCTGTATGAAAGCAGGCATCTAAGGAGCAGATTGGAATTAAA 2707
2708  AACAACTGTTCAGTGAAAAAAAAAAAAAA                                                                                  2736
```

Figure 2. Nucleotide and deduced amino acid sequences of rat M-cadherin. The deduced amino acid sequence is shown below the nucleotide sequence. The stop codon is denoted by an asterisk. The signal peptide is in blue and the postulated furin cleavage site of the precursor polypeptides is indicated by a ^. The extracellular domain is divided into five cadherin extracellular subdomain repeats (*EC1-EC5*). The transmembrane domain is in green. In the cytoplasmic domain following the transmembrane domain, the membrane-proximal conserved domain (MPCD) is in purple and the catenin binding sequence (CBS) is in orange. The characteristic cadherin consensus sequences are shaded in red. The 4 cysteine residues in EC5 are in pink. The *N*-glycosylation sites are indicated in brown. The nucleotide sequence of rat M-cadherin is in GenBank with the accession number AB176538.

The expression level of rat M-cadherin was compared between TR-iBRB and TR-BBB cells. Following quantitative real time PCR analysis using rat M-cadherin specific primers amplified at nucleotide position 790-916, the rat M-cadherin mRNA content relative to the amount of GAPDH mRNA (M-cadherin/GAPDH) in TR-iBRB2, TR-iBRB9, TR-BBB11, and TR-BBB13 cells was $2.38\pm0.41\times10^{-3}$, $6.93\pm0.67\times10^{-3}$, $7.32\pm4.80\times10^{-5}$, and $2.74\pm0.49\times10^{-5}$, respectively (Figure 3A). The mean value of the rat M-cadherin mRNA content in TR-iBRB cells was 92.9 fold greater than that in TR-BBB cells. Consistent with mRNA expression, immunoblot analysis revealed that the expression of rat M-cadherin protein at 130 kDa in TR-iBRB cells was greater than that in TR-BBB cells (Figure 3B). The molecular weight of rat M-cadherin at 130 kDa was identical to the reported value for rat L6 myoblasts [14].

## DISCUSSION

This study found eight genes expressed more in retina than in brain capillary endothelial cell lines using mRNA differential display analysis with 48 primer combinations (Table 1). Three hundred primer combinations are required to visualize all differentially displayed genes [15]. Therefore, 16% of mRNAs in both cell lines were screened in this study, and further 42 genes are expected to exist as a differentially displayed gene in TR-iBRB cells. For the analysis of differentially displayed genes between the inner BRB and BBB, it is important to use cells exhibiting normal physiological properties. In the case of isolated capillary endothelial cells from animals, it is difficult to avoid contamination from non-endothelial cells and obtain a sufficient number of cells due to very small dimensions of the retina. Using TR-iBRB and TR-BBB cells eliminates these concerns, since both cell lines were established from the same rat strain using the same procedure and cultured in the same conditions. Moreover, both cell lines possess the same endothelial markers and express several transporters [9-11], which have been reported to be expressed in vivo retinal and brain capillaries [2,3,6,7]. Therefore, the difference in expressed genes between these cell lines may indeed reflect the difference between the inner BRB and BBB in vivo.

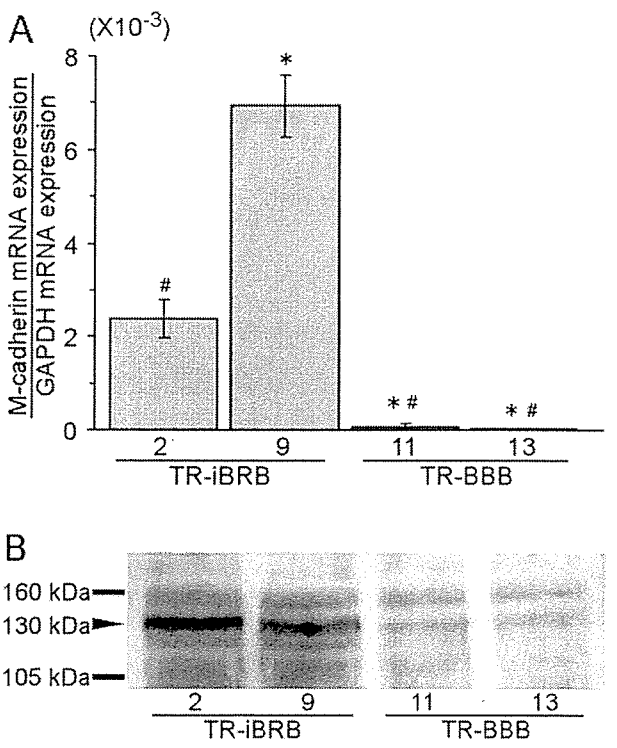


Figure 3. Expression of rat M-cadherin in TR-iBRB and TR-BBB cells. **A**: Quantitative real time PCR analysis of rat M-cadherin. The rat M-cadherin mRNA expression level was normalized by the GAPDH mRNA expression. Each point represents the mean of 3-4 observations. The error bars represent the standard error of the mean. An asterisk ("*") indicates $p<0.01$ for the comparison to TR-iBRB2 cells. A sharp sign ("#") indicates $p<0.01$ for the comparison to TR-iBRB9 cells. **B**: Immunoblot analysis of rat M-cadherin. One representative immunoblot analysis from three independent experiments is shown.

Cadherin is an adherens junction protein and mediates calcium dependent cell-cell adhesion in a homophilic manner [16]. It has been reported that some cadherin-family proteins are expressed at the inner BRB and the BBB. VE-Cadherin (cadherin-5), an endothelial cell specific protein which is necessary for vessel formation in vivo [17], is localized to adhesion sites of endothelial cells in the retina and brain [18,19]. In embryonic chicken brain and retina, N-cadherin (cadherin-2) is expressed at contact zones between pericytes and endothelial cells and its concentration rapidly falls with the onset of barrier differentiation, suggesting that N-cadherin expression represents a signal for the expression of barrier properties [20]

The present study revealed that M-cadherin is highly expressed in TR-iBRB cells, but not in TR-BBB cells (Figure 3). TR-BBB cells originate from the cerebrum, and there is no report of M-cadherin being expressed in the cerebrum. On the other hand, when *nls-lacZ* reporter gene was introduced into the M-cadherin locus, strong β-gal activity was observed in the distinct cell layer of the retina [21], suggesting that M-cadherin is expressed in the retina. Ultrastructural comparison between the retinal and brain capillaries shows that retinal vessels have denser interendothelial junctions and a greater covering of pericytes than brain vessels [1]. In diabetes, the neovascularization following the loss of pericytes from vessels mostly occurs in the inner BRB, and may not take place in the BBB [22]. It is proposed that M-cadherin is intimately involved in these ultrastructural and pathological differences in cell-cell adhesion between the inner BRB and BBB.

Rat M-cadherin, which has been cloned for the first time, contains a hydrophobic signal sequence at amino acids 1-21 [23] and a postulated furin cleavage site of precursor polypeptides at amino acids 44-45 [23]. The deduced 740 amino acid sequence of mature M-cadherin protein consists of a long extracellular domain containing five cadherin extracellular subdomain repeats (EC1-EC5), a transmembrane domain, and a cytoplasmic domain. The extracellular domain of M-cadherin

includes the characteristic cadherin consensus sequences DXD, LD(R/Y)E, and DXNDNXP which are involved in $Ca^{2+}$ binding [24]. Furthermore, four cysteine residues conserved in cadherin are also present in the EC5 of M-cadherin. There are five *N*-glycosylation sites in the extracellular domain. The cytoplasmic domain of M-cadherin includes a membrane-proximal conserved domain (MPCD) [16], which is implicated in the basolateral sorting of cadherin molecules, and a catenin binding sequence (CBS) [16].

The 3' termini of GATA-3 and BCATc mRNAs were expressed 24 and 5.5 fold more in TR-iBRB than TR-BBB cells, respectively. A transcription factor, GATA-3, is predominantly expressed and required for optimal cytokine production in T helper type 2 cells [25]. Although the physiological role of GATA-3 at the inner BRB is not clear at the present time, GATA-3 may regulate the expression of some genes that are responsible for the unique functions of the inner BRB. Branched chain amino transferase (BCAT) is involved in de novo glutamate synthesis by transferring nitrogen from the branched-chain amino acids to α-ketoglutarate and vice versa primarily in the retina and the brain [26]. BCATc is proposed to play a more important role in de novo glutamate synthesis at the inner BRB than the BBB. This was supported by the finding that the percentages of glutamate input into the glutamate/glutamine cycle, which are provided by de novo glutamate synthesis, are about 30% and 20% in the retina and whole brain, respectively [26]. Further studies are needed to understand these functions in the retina in vivo. It is important to investigate whether other clones with an expression ratio between 2 and 5 (clones 5, 6, 7, and 8) reflect differences in the two tissues. This confirms that mRNA differential display analysis using both cell lines is a useful technique to determine differences in gene expression between the inner BRB and BBB.

In conclusion, eight clones were identified as highly expressed genes in TR-iBRB cells compared with TR-BBB cells using mRNA differential display analysis. Of these eight clones, M-cadherin, GATA-3, and BCATc were more abundantly expressed in TR-iBRB cells than TR-BBB cells and may indeed be involved in unique functions at the inner BRB. Moreover, rat M-cadherin gene, which has been cloned from TR-iBRB cells, for the first time, was expressed to a much greater extent in TR-iBRB than in TR-BBB and may be responsible for some cell-cell adhesion differences between the two tissues. The selective expression of genes at the inner BRB compared with the BBB may have important implications for the unique function of the inner BRB and the retina.

## ACKNOWLEDGEMENTS

The authors thank Drs. Tadahiro Oshida, Hideaki Takeuchi, and Gozo Tsujimoto for valuable discussions. This study was supported, in part, by a Grant in Aid for Scientific Research from the Japan Society for the Promotion of Science.

## REFERENCES

1. Stewart PA, Tuor UI. Blood-eye barriers in the rat: correlation of ultrastructure with function. J Comp Neurol 1994; 340:566-76.
2. Holash JA, Stewart PA. The relationship of astrocyte-like cells to the vessels that contribute to the blood-ocular barriers. Brain Res 1993; 629:218-24.
3. Takata K, Kasahara T, Kasahara M, Ezaki O, Hirano H. Ultracytochemical localization of the erythrocyte/HepG2-type glucose transporter (GLUT1) in cells of the blood-retinal barrier in the rat. Invest Ophthalmol Vis Sci 1992; 33:377-83.
4. Nakashima T, Tomi M, Katayama K, Tachikawa M, Watanabe M, Terasaki T, Hosoya K. Blood-to-retina transport of creatine via creatine transporter (CRT) at the rat inner blood-retinal barrier. J Neurochem 2004; 89:1454-61.
5. Ohtsuki S, Tachikawa M, Takanaga H, Shimizu H, Watanabe M, Hosoya K, Terasaki T. The blood-brain barrier creatine transporter is a major pathway for supplying creatine to the brain. J Cereb Blood Flow Metab 2002; 22:1327-35.
6. Pardridge WM, Boado RJ, Farrell CR. Brain-type glucose transporter (GLUT-1) is selectively localized to the blood-brain barrier. Studies with quantitative western blotting and in situ hybridization. J Biol Chem 1990; 265:18035-40.
7. Schinkel AH, Smit JJ, van Tellingen O, Beijnen JH, Wagenaar E, van Deemter L, Mol CA, van der Valk MA, Robanus-Maandag EC, te Riele HP, Berns AJ, Borst P. Disruption of the mouse mdr1a P-glycoprotein gene leads to a deficiency in the blood-brain barrier and to increased sensitivity to drugs. Cell 1994; 77:491-502.
8. Hosoya K, Saeki S, Terasaki T. Activation of carrier-mediated transport of L-cystine at the blood-brain and blood-retinal barriers in vivo. Microvasc Res 2001; 62:136-42.
9. Hosoya KI, Takashima T, Tetsuka K, Nagura T, Ohtsuki S, Takanaga H, Ueda M, Yanai N, Obinata M, Terasaki T. mRna expression and transport characterization of conditionally immortalized rat brain capillary endothelial cell lines; a new in vitro BBB model for drug targeting. J Drug Target 2000; 8:357-70.
10. Hosoya K, Tomi M, Ohtsuki S, Takanaga H, Ueda M, Yanai N, Obinata M, Terasaki T. Conditionally immortalized retinal capillary endothelial cell lines (TR-iBRB) expressing differentiated endothelial cell functions derived from a transgenic rat. Exp Eye Res 2001; 72:163-72.
11. Terasaki T, Ohtsuki S, Hori S, Takanaga H, Nakashima E, Hosoya K. New approaches to in vitro models of blood-brain barrier drug transport. Drug Discov Today 2003; 8:944-54.
12. Donalies M, Cramer M, Ringwald M, Starzinski-Powitz A. Expression of M-cadherin, a member of the cadherin multigene family, correlates with differentiation of skeletal muscle cells. Proc Natl Acad Sci U S A 1991; 88:8024-8.
13. Shimoyama Y, Shibata T, Kitajima M, Hirohashi S. Molecular cloning and characterization of a novel human classic cadherin homologous with mouse muscle cadherin. J Biol Chem 1998; 273:10011-8.
14. Zeschnigk M, Kozian D, Kuch C, Schmoll M, Starzinski-Powitz A. Involvement of M-cadherin in terminal differentiation of skeletal muscle cells. J Cell Sci 1995; 108:2973-81.
15. Guimaraes MJ, Lee F, Zlotnik A, McClanahan T. Differential display by PCR: novel findings and applications. Nucleic Acids Res 1995; 23:1832-3.
16. Nollet F, Kools P, van Roy F. Phylogenetic analysis of the cadherin superfamily allows identification of six major subfamilies besides several solitary members. J Mol Biol 2000; 299:551-72.
17. Vittet D, Buchou T, Schweitzer A, Dejana E, Huber P. Targeted null-mutation in the vascular endothelial-cadherin gene impairs the organization of vascular-like structures in embryoid bodies. Proc Natl Acad Sci U S A 1997; 94:6273-8.
18. Breier G, Breviario F, Caveda L, Berthier R, Schnurch H, Gotsch

U, Vestweber D, Risau W, Dejana E. Molecular cloning and expression of murine vascular endothelial-cadherin in early stage development of cardiovascular system. Blood 1996; 87:630-41.
19. Russ PK, Davidson MK, Hoffman LH, Haselton FR. Partial characterization of the human retinal endothelial cell tight and adherens junction complexes. Invest Ophthalmol Vis Sci 1998; 39:2479-85.
20. Gerhardt H, Liebner S, Redies C, Wolburg H. N-cadherin expression in endothelial cells during early angiogenesis in the eye and brain of the chicken: relation to blood-retina and blood-brain barrier development. Eur J Neurosci 1999; 11:1191-201.
21. Hollnagel A, Grund C, Franke WW, Arnold HH. The cell adhesion molecule M-cadherin is not essential for muscle development and regeneration. Mol Cell Biol 2002; 22:4760-70.
22. Kern TS, Engerman RL. Capillary lesions develop in retina rather than cerebral cortex in diabetes and experimental galactosemia. Arch Ophthalmol 1996; 114:306-10.
23. Nielsen H, Engelbrecht J, Brunak S, von Heijne G. Identification of prokaryotic and eukaryotic signal peptides and prediction of their cleavage sites. Protein Eng 1997; 10:1-6.
24. Overduin M, Harvey TS, Bagby S, Tong KI, Yau P, Takeichi M, Ikura M. Solution structure of the epithelial cadherin domain responsible for selective cell adhesion. Science 1995; 267:386-9.
25. Pai SY, Truitt ML, Ho IC. GATA-3 deficiency abrogates the development and maintenance of T helper type 2 cells. Proc Natl Acad Sci U S A 2004; 101:1993-8.
26. Lieth E, LaNoue KF, Berkich DA, Xu B, Ratz M, Taylor C, Hutson SM. Nitrogen shuttling between neurons and glial cells during glutamate synthesis. J Neurochem 2001; 76:1712-23.

The print version of this article was created on 9 Aug 2004. This reflects all typographical corrections and errata to the article through that date. Details of any changes may be found in the online version of the article.

*Molecular Vision* 2004; 10:618-28 <http://www.molvis.org/molvis/v10/a74>
Received 11 December 2003 | Accepted 29 August 2004 | Published 30 August 2004



# Downregulation of retinal GLUT1 in diabetes by ubiquitinylation

**Rosa Fernandes,[1,2] Ana Luisa Carvalho,[3] Arno Kumagai,[2] Raquel Seica,[4] Ken-ichi Hosoya,[5] Tetsuya Terasaki,[6] Joaquim Murta,[1] Paulo Pereira,[1] Carlos Faro[7]**

*[1]Biomedical Institute for Research in Light and Image, Center of Ophthalmology, University of Coimbra, Coimbra, Portugal; [2]Department of Internal Medicine and the Juvenile Diabetes Research Foundation (JRDF) Center for Complications in Diabetes, University of Michigan Medical School, Ann Arbor, MI; [3]Department of Zoology, [4]Faculty of Medicine, and [7]Department of Biochemistry, Center for Neuroscience, University of Coimbra, Coimbra, Portugal; [5]Faculty of Pharmaceutical Sciences, Toyama Medical and Pharmaceutical University, 2630 Sugitani, Toyama, Japan; [6]Graduate School of Pharmaceutical Sciences, Tohoku University, Aoba, Aramaki, Aoba-ku, Sendai, Japan*

**Purpose:** To investigate the effect of chronic hyperglycemia on the levels of the glucose transporter GLUT1 in retina and its ubiquitinylation.

**Methods:** Two diabetic animal models (Goto Kakizaki rats and alloxan-induced diabetic rabbits) and retinal endothelial cells in culture were used. GLUT1 content was determined by western blotting. Glut1 mRNA was determined by RT-PCR and northern blotting. Ubiquitin conjugates were evaluated by western blot analysis. In vitro ubiquitin conjugation activity was evaluated in supernatants using radiolabeled ubiquitin. Evidence for GLUT1 ubiquitinylation was further investigated by transfecting HEK293 cells with a hemagglutinin (HA)-tagged ubiquitin cDNA followed by immunoprecipitation of the cell lysates.

**Results:** Chronic hyperglycemia resulted in a significant decrease on the amount of GLUT1 protein without significant changes on the GLUT1 mRNA in the retinas of diabetic GK rats and alloxan treated rabbits, and in high glucose treated retinal endothelial cells, compared to controls. The content of high molecular weight ubiquitin conjugates was higher both in the membrane fractions of diabetic retinas and in endothelial cells incubated with high glucose concentrations. GLUT1 immunoprecipitated from diabetic retinas crossreacted with antibodies directed against ubiquitin suggesting that GLUT1 is posttranslationally modified by monoubiquitinylation. Cells transfected with HA-tagged ubiquitin revealed crossreactivity with anti-GLUT1 antibodies on the HA immunoprecipitates.

**Conclusions:** The data indicate that retinal GLUT1 abundance decreases in experimental diabetes and with exposure of retinal endothelial cells to elevated glucose concentrations. Results further suggest that decreased abundance of GLUT1 may be associated with its increased degradation by a ubiquitin dependent mechanism. Ubiquitinylation of GLUT1 may be the mechanism targeting GLUT1 for degradation in diabetes.

Hyperglycemia is considered the major determinant of vascular complications and development of diabetic retinopathy. The molecular mechanisms underlying such changes are poorly understood. Nevertheless, there are some pathways proposed to be involved in glucose toxicity, including nonenzymatic glycation, activation of protein kinase C, and increased production of reactive oxygen species combined with impaired antioxidative defenses [1,2]. In addition to nutrient supply, the capillaries of the retina constitute a barrier to the passage of blood-borne compounds and solutes between the blood and the retina. In the inner retina, this barrier is comprised of microvascular endothelial cells and is known as the inner blood-retinal barrier (BRB). The outer retina possesses another barrier, the outer BRB, that consists of the retinal pigment epithelial cells. Due to the presence of the BRB, glucose cannot freely pass from blood to the retina. Glucose transport across this barrier is mediated by a facilitative transporter, GLUT1 [3].

Correspondence to: Paulo Pereira, Department of Ophthalmology, IBILI Azinhaga de Santa Comba, Celas, 3000-354, Portugal; Phone: (351) 239480225; FAX: (351) 239480280; email: ppereira@imagem.ibili.uc.pt

The regulation of GLUT1 in retinal endothelial cells in response to chronic hyperglycemia is not clear. There are conflicting data concerning the effect of hyperglycemia on glucose transport and on GLUT1 expression. In a diabetic animal model, Badr and colleagues showed a decrease of approximately 50% in whole retinal GLUT1 and retinal microvascular GLUT1, for 8 week-long diabetes [4]. Mandarino et al [5] reported an unchanged uptake of 3-O-methylglucose (3-OMG) in high glucose treated bovine retinal endothelial cells compared with pericytes, which showed a downregulation in 3-OMG uptake. In contrast, very recently, Busik et al [6] showed an increase of glucose uptake in human retinal vascular endothelial cells incubated under high glucose, without a change in endothelial cell GLUT1.

The effect of diabetes on expression and regulation of the GLUT1 glucose transporter in endothelial cells is evaluated in this study. To investigate the regulation of GLUT1 levels in BRB in response to hyperglycemia, we used two diabetic animal models and retinal endothelial cells. We demonstrate that GLUT1 conjugation with ubiquitin may constitute a posttranslational mechanism through which the cellular levels of GLUT1 are regulated under hyperglycemia.

## METHODS

*Animals:* In this study two diabetic animal models were used, the Goto Kakizaki (GK) rats and the alloxan-induced diabetic rabbits. Wistar and GK rats were obtained from a local breeding colony maintained at the University Hospitals of Coimbra. After 6 weeks of age, the GK rats showed persistent hyperglycemia. Six month old and one year old diabetic and age matched nondiabetic Wistar control rats were used in these experiments. The rats were fed normal rat chow ad libitum and maintained in temperature-controlled facilities with 12 h light-dark cycles. Glucose concentrations were measured on tail blood samples using a glucose monitor (Gluco Touch; Lifescan, Milpitas, CA).

Diabetes in rabbits was induced by the injection of a freshly prepared solution of alloxan in serum at a dose of 110 mg/kg body in a prominent ear vein. A sample of blood was obtained weekly from the ear vein to monitor glucose concentrations.

All animals were handled in accordance with ARVO Statement for the use of Animals in Opththalmic and Vision Research.

Rats and rabbits were sacrificed by decapitation and their eyes were quickly removed. Retinas were isolated and wrapped in aluminum foil, frozen on liquid nitrogen and stored at -80 °C until used.

*Primary cell cultures of bovine retinal endothelial cells:* Bovine retinas were the source of capillaries used to isolate cells for primary culture. Cow eyes were obtained from a local abattoir. Primary bovine retinal endothelial cells (BREC) cultures were established from fresh calf eyes. Under sterile conditions, the retinas were isolated and washed in Dulbecco's modified Eagle's medium (DMEM; Invitrogen, Carlsbad, CA) and pieces of adherent retinal pigment epithelial cells were removed. The retinas were transferred to an enzyme solution containing pronase (100 μg/ml; Roche, Mannheim, Germany), collagenase (500 μg/ml; Invitrogen) and DNase (70 μg/ml; Sigma-Aldrich, St. Louis, MO) and incubated with shaking at 37 °C for 20 min. After incubation, the retinal digest was passed through 210 and 50 μm nylon mesh and the microvessels trapped on top of the 50 μm mesh were collected in DMEM by centrifugation. The fragments were resuspended in DMEM with 15% fetal calf serum (FCS), 20 μg/ml endothelial growth supplement (Roche, Mannheim, Germany), heparin (100 μg/ml) and antibiotic-antimycotic solution (Sigma, St. Louis, MO), plated and grown on fibronectin coated dishes in low glucose DMEM, at 37 °C with 5% $CO_2$.

To determine the effect of high glucose on GLUT1 expression, BREC were grown in low (5.5 mM) or high (25 mM) D-glucose medium up to 48 h.

*Cell line of retinal capillary endothelial cells:* A conditionally immortalized retinal capillary endothelial cell line (TR-iBRB) [7] was grown and maintained in DMEM with low glucose, containing 10% fetal bovine serum (FBS; Gibco BRL Life Technologies, Inchiman, UK), 100 U/ml penicillin G, 100 U/ml streptomycin (Sigma), in a humidified atmosphere composed of 95% air and 5% $CO_2$ at 33 °C. Cells were grown to approximately 40-50% confluence and incubated in regular DMEM containing 5.5 or 25 mM glucose at 37 °C. Control experiments using mannitol were performed to test the effect of high osmolarity on the GLUT1 expression. There were no changes in the GLUT1 expression in cells treated with 25 mM mannitol for 48 h.

Human embryonic kidney (HEK)293 cells were cultured in DMEM supplemented with 10% FBS, 100 U/ml penicillin G, 100 U/ml streptomycin, in a humidified atmosphere composed of 95% air and 5% $CO_2$ at 37 °C.

*Antibodies:* Goat polyclonal antibody raised against the COOH terminus of rabbit GLUT1 was purchased from Santa Cruz Biotechnology, Inc. (Santa Cruz, California). Rabbit polyclonal antibody raised against purified human erythrocyte GLUT1 was a kind gift from Christin Carter-Su. Monoclonal anti-ubiquitin antibody was purchased from Affiniti Research Products Ltd. (Mamhead Castle, UK) and polyclonal anti-ubiquitin antibody was a kind gift from Dr. Fu Shang (Tufts University, Boston, MA). Mouse monoclonal antibody against actin was purchased from Boehringer Mannheim (Mannheim, Germany). Polyclonal anti-hemagglutinin antibody was purchased from Zymed Laboratories Inc. (South San Francisco, CA).

**Table 1. Body weight and plasma glucose levels for control (Wistar) and diabetic (GK) rats**

| | n | Body weight (g) | Serum glucose (mg/dL) |
|---|---|---|---|
| Wistar rats | | | |
| 6 months | 5 | 552±40 | 121± 6 |
| 12 months | 4 | 811±42 | 91± 7 |
| GK rats | | | |
| 6 months | 4 | 367±14* | 267±34* |
| 12 months | 4 | 423±52* | 329±25* |

Values in table are means±standard error. An asterisk (*) indicates a stastically significant difference ($p<0.01$) between diabetic (GK) and age matched control (Wistar) rats.

**Table 2. Body weight and plasma glucose levels for nondiabetic and diabetic rabbits**

| | n | Body weight (g) | Serum glucose (mg/dL) |
|---|---|---|---|
| Control | 5 | 2420± 79 | 102± 3 |
| Diabetic | | | |
| 2 weeks | 6 | 2575± 80 | 365±39 |
| 2 months | 7 | 3097±198 | 378±48 |
| 4 months | 7 | 3668± 95 | 332±27 |

Values in table are means±standard error. There were statistically significant differences ($p<0.01$) for measurements of body weight and serum glucose between diabetic (alloxan-induced) rabbits and control rabbits.

*Isolation of the membrane fraction from the retina of diabetic and control animals:* Total retina homogenates from diabetic or control animals were obtained by tissue lysis in 10 mM Tris-HCl, 1 mM EDTA, 250 mM sucrose, protease inhibitors, pH 7.4, at 4 °C and mechanical disruption using a Potter-Elvehjem homogenizer (50-60 strokes). The samples were centrifuged at 900x g to remove nuclei, mitochondria and unlysed cells, and recentrifuged at 100,000x g for 75 min to obtain the total cell membranes. The membrane pellet was resuspended in 10 mM Tris-HCl, 1 mM EDTA, pH 7.4 containing protease inhibitors, 0.5% sodium deoxycholate (DOC) and 1% TritonX-100. The samples were then centrifuged at 14,000x g to remove the unsoluble fraction. The protein concentration was measured using the BCA reagent (Pierce, Rockford, IL) with BSA as the standard.

*Extracts from retinal endothelial cells (BREC and TR-iBRB cells):* After incubation with glucose, the BREC and TR-iBRB cells were washed twice with ice-cold PBS and then lysed with 10 mM Tris-HCl, 1 mM EDTA, pH 7.4 containing protease inhibitors, 0.5% DOC and 1% Triton X-100. The lysates were sonicated 6 times for 3 s and then centrifuged at 14,000x g for 15 min. The supernatants were used to determine the protein concentration and were then denaturated with Laemmli buffer.

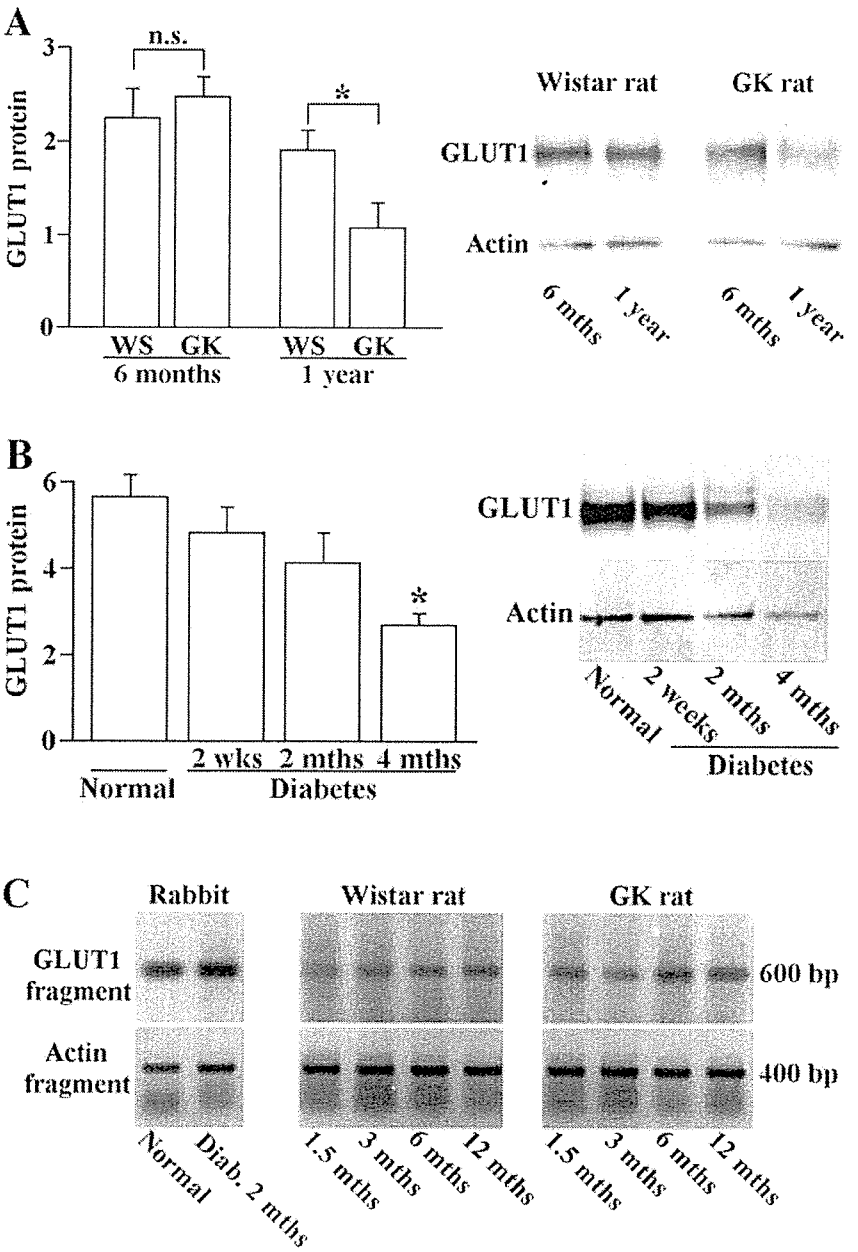


Figure 1. Effect of diabetes on GLUT1 expression in retina. **A**: GLUT1 protein expression in retina from 1 year old non-diabetic rats is greater than in age matched diabetic GK rats. Membrane fractions were isolated from rat retinas. Equal amounts of protein (30 μg) were subjected to immunoblotting and membranes were probed with anti-GLUT1 antibodies. Actin expression on the same membrane is included to demonstrate comparable loading of lanes. Graphical summary and western blots are provided. Bars represent standard errors (4 rats/group). The asterisk (*) indicates that the GLUT1 protein expression for 1 year old diabetic GK rats are stastically different from the age matched control Wistar rats ($p<0.05$). **B**: GLUT1 protein expression in diabetic rabbit retinas is decreased compared to controls. The duration of diabetes was 2 weeks, 2 and 4 months. Membrane fractions were isolated from rabbit retinas. Equal amounts of protein (5 μg) were subjected to immunoblotting and probed with antibodies directed against GLUT1 and actin. Western blots are provided. The graphic represents the results normalized for actin. Bars represent standard errors (5 rabbits/group). The asterisk (*) indicates that the GLUT1 protein expression for rabbits with-diabetes for 4 months are significantly different from the the control rabbits ($p<0.01$). **C**: Slight increase on retinal GLUT1 mRNA levels in diabetic animals. Total retinal RNA (1 μg or 150 ng) was subjected to RT-PCR analysis for determination of GLUT1 and actin mRNA levels.

*Isolation of total RNA from retina and TR-iBRB cells:* Total RNA was isolated from rat and rabbit retinas using TRIzol® Reagent (Gibco BRL, Paisley, UK), according to manufacturer's protocol. Briefly, tissues were homogenized in guanidium isothiocyanate and phenol. Chloroform extraction allowed recovery of RNA in the aqueous phase. The RNA was then precipitated with isopropyl alcohol, and the RNA pellet was washed with 75% ethanol and redissolved in DEPC treated water. Total RNA samples were treated with RNase-free DNase prior to reverse transcription to ensure that the samples were free of contaminating DNA.

Total RNA from TR-iBRB cells was isolated using the RNeasy mini kit (Qiagen, Valencia, CA) according to the manufacturer's protocol.

The total amount of RNA was quantified by optical density (OD) measurements at 260 nm and the purity was evaluated by measuring ratio of OD at 260 and 280 nm.

*Western blotting:* For the western blot analysis, 5 to 30 μg protein were loaded per lane on sodium dodecyl sulphate-polyacrylamide gels (SDS-PAGE). Following electrophoresis and transfer to polyvinylidene fluoride (PVDF) membranes (Boehringer Mannheim), the blots were incubated in Tris buffered saline (20 mM Tris, 137 mM NaCl, pH 7.6) containing 0.1% Tween 20 (TBST), and 5% nonfat milk for 1 h. Membranes were then incubated with 1:1,000 dilution of affinity-purified goat polyclonal anti-GLUT1 (Santa Cruz Biotechnology, Inc.), 1:10,000 dilution of rabbit polyclonal antibody against GLUT1, 1:10,000 dilution of the anti-actin antibody, or 1:1,000 dilution of mouse monoclonal (FK2) or polyclonal antibodies to ubiquitinylated proteins, for 1 h 30 min, in TBST containing 0.5% non fat milk. After five washes with TBST, blots were reacted for 1 h with 1:10,000 dilution of secondary antibodies coupled to alkaline-phosphatase in TBST containing 0.5% nonfat milk, and were then washed 5 times with TBST and were developed using an enhanced fluorescence kit (Amersham Pharmacia Biotech, Buckinghamshire, UK). Blots were scanned in the Storm 860 (Molecular Dynamics, Amersham Biosciences, Uppsala, Sweden) and the optical density of the bands was measured with Image Quant 5.0 Software (Molecular Dynamics). The intensity of the GLUT1 bands was normalized for every sample relatively to the intensity of the respective actin bands.

*Determination of ubiquitin conjugating activity:* The ability of TR-iBRB or retina supernatants to catalyse the conjugation of exogenous radiolabeled ubiquitin ($^{125}$I) to endogenous proteins was determined using an assay modified from Hershko et al [8]. Briefly, cells or retinas were sonicated in 50 mM Tris-HCl buffer, pH 7.6. The lysates were centrifuged at 14,000x g during 10 min, at 4 °C. Reactions were performed in a final volume of 25 μl, containing 15 μl of supernatant (80 μg of TRi-BRB cell supernatant lysates or 50 μg of retina supernatant lysates), 10 μl of conjugation buffer solution (50 mM Tris-HCl, pH 7.6, 5 mM $MgCl_2$, 1 mM DTT, 2 mM ATP, 34.8 U/ml creatine phosphokinase, 10 mM creatine phosphate) and 0.3 μg of $^{125}$I-ubiquitin (approximately 2 x $10^5$ c.p.m). Controls were generated by incubation with buffer A (50 mM Tris-HCl, pH 7.6, 5 mM $MgCl_2$ and 1 mM DTT). After 20 min of incubation at 37 °C, the reaction was terminated by the addition of 25 μl of 2X Laemmli buffer followed by at least 30 min at room temperature. Aliquots of the assays were separated by SDS/12%-PAGE. Autoradiograms of dried gels were obtained and scanned for densitometric analysis.

*Northern blotting:* Total RNA was isolated from control and high glucose treated TR-iBRB cells. Aliquots (20 μg) of total RNA were loaded on a 2 M formaldehyde 1% agarose gel, and run overnight at 20 V. RNA was then transferred to a nylon membrane (Schleicher & Schuell BioScience, Inc., Keene, NH) by capillary action for about 24 h. Northern blot analysis for GLUT1 and mouse actin were performed as previously described [9], using a 512 kb *PstI* fragment of the bovine blood-brain barrier glucose transporter cDNA [10] linearized with *Hind*III, and a mouse actin clone, pAM-91 (generously provided by Michael J. Getz, Mayo Clinic/Foundation, Rochester, MI), linearized with *EcoR*I. Both cDNAs were labeled with [$^{32}$P]-dCTP using a random primer method, as described previously [9]. Quantification of autoradiograms was performed using NIH Image software (version 1.6) and the GLUT1 signal was normalized against the signal for actin.

*Semi quantitative RT-PCR analyses:* GLUT1 mRNA levels were determined by quantitative reverse transcription-PCR

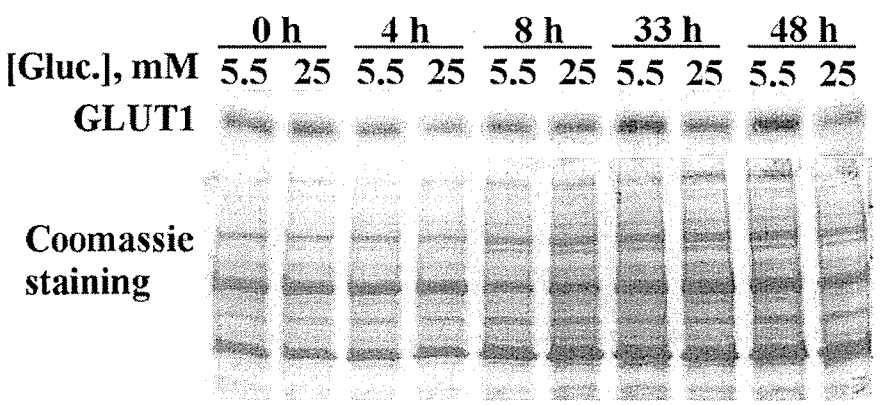


Figure 2. Effect of high glucose on GLUT1 expression in primary cultures of BREC cells. In BREC cells exposed to high glucose concentration there is a decrease in the amount of GLUT1 protein. The cells were solubilized in Laemmli buffer without β-Mercaptoethanol and equal amounts of protein (30 μg) were loaded on a 12% polyacrylamide gel following addition of reducing agent β-Mercaptoethanol. The proteins were resolved by SDS-PAGE, transferred to PVDF membrane and probed with an antiserum against GLUT1. Coomassie staining is used as a control for total protein loading.

of total RNA from retinas, using the forward primer 5'-CTC CAC GAG CAT CTT CGA GAA G-3' and the reverse primer 5'-TCA CAC TTG GGA ATC AGC CC-3' for amplification of GLUT1, and the forward primer 5'-GAC TAC CTC ATG AAG ATC CT-3' and the reverse primer 5'-ATC TTG ATC TTC ATG GTG CTG-3' for amplification of actin.

For the RT-PCR reactions, 150 ng or 1 μg of total RNA from rabbits and rats retinas, respectively, were used for GLUT1 and actin amplification. Amplification products were electrophoresed on 1% agarose gels and stained with ethidium bromide. The gel was then photographed on a UV transiluminator.

*Transfection:* HEK293 cells were transiently transfected with the plasmid encoding hemagglutinin-tagged ubiquitin, under the control of the CMV promoter, which was kindly donated by Dr. Bohmann, University of Rochester, Rochester, NY. The transfection was carried out using LipofectAMINE™ (Gibco BRL). Cells were incubated with plasmid DNA for 6 h, and the same volume of fresh medium, containing 10% FBS, was then added to the cells. Cells were used 24 h after transfection.

*Immunoprecipitation:* Immunoprecipitations were performed by incubation of the protein extracts from retinas or cells with the anti-GLUT1 (2.5 μg) or anti-HA (3.75 μg) antibodies, overnight at 4 °C. The protein-antibodies complexes were collected on protein G-Sepharose or protein A-Sepharose beads. The beads were extensively washed and the immunoprecipitated proteins were eluted in Laemmli buffer and resolved by SDS-PAGE.

*Statistical analysis:* Measurements of the GLUT1 expression levels were averaged for each group of animals. A minimum of three northern blot analysis was done for each group of animals and a minimum of four measurements of GLUT1 protein expression by western blot analysis was performed. The mean values from each group were then used to compute an overall mean and standard error of the mean. Comparisons between groups were made with an unpaired two tailed Student's t-test. The $\alpha$ level for statistical significance was set at 0.05.

## RESULTS

*Animal and cell models of diabetes:* To establish the effect of hyperglycemia on the expression of GLUT1, the level of GLUT1 was analysed in two diabetic animal models and compared to the level of expression of GLUT1 in control animals.

One of the diabetic animal models used was the GK rat, which spontaneously develops non-insulin-dependent *type 2* diabetes. These animals begin to develop chronic hyperglycemia at 4 to 6 weeks of age [11] which remains stable during ageing of the animals. Associated with hyperglycemia, these animals present hyperinsulinemia, glucose intolerance and some of the metabolic and anatomic changes similar to those observed in human diabetic retinopathy [12-14]. The GK rats were produced by selective breeding of normal Wistar rats

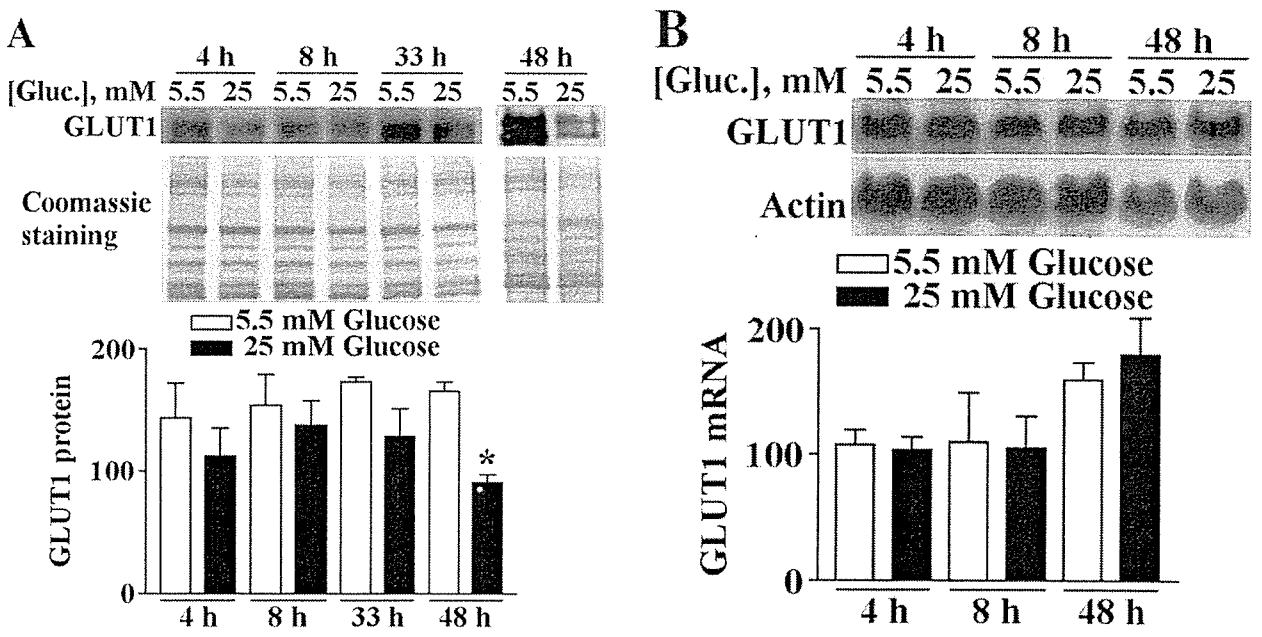


Figure 3. Effect of high glucose on expression of GLUT1 in TR-iBRB cells. **A**: In TR-iBRB cells exposed to high glucose concentration there is a subnormal expression of GLUT1 protein. The cells were solubilized in SDS-PAGE buffer and equal amounts of protein (30 μg) were loaded on a 12% polyacrylamide gel. The proteins were resolved by SDS-PAGE, transferred to PVDF membrane and probed with an antiserum against GLUT1. Bars represent standard errors (3 rats/group). The asterisk (*) indicates $p<0.05$. **B**: There are no significant changes in the levels of GLUT1 mRNA after 48 h of hyperglycemia. The total RNA was isolated from control and high glucose treated TR-iBRB cells and northern blot analysis was performed. Bars represent standard errors (3 rats/group).

and therefore the Wistar rats are considered appropriate controls since these two groups of animals have the same genetic background [11,15]. The second diabetic animal model used was the alloxan treated rabbit that mimics *type 1* diabetes. Several reports showed retinal abnormalities such as microaneurysms, pericyte loss, acellular capillaries [16] and ultrastructural disorders of vessels and basement membrane [17] in alloxan-induced diabetes.

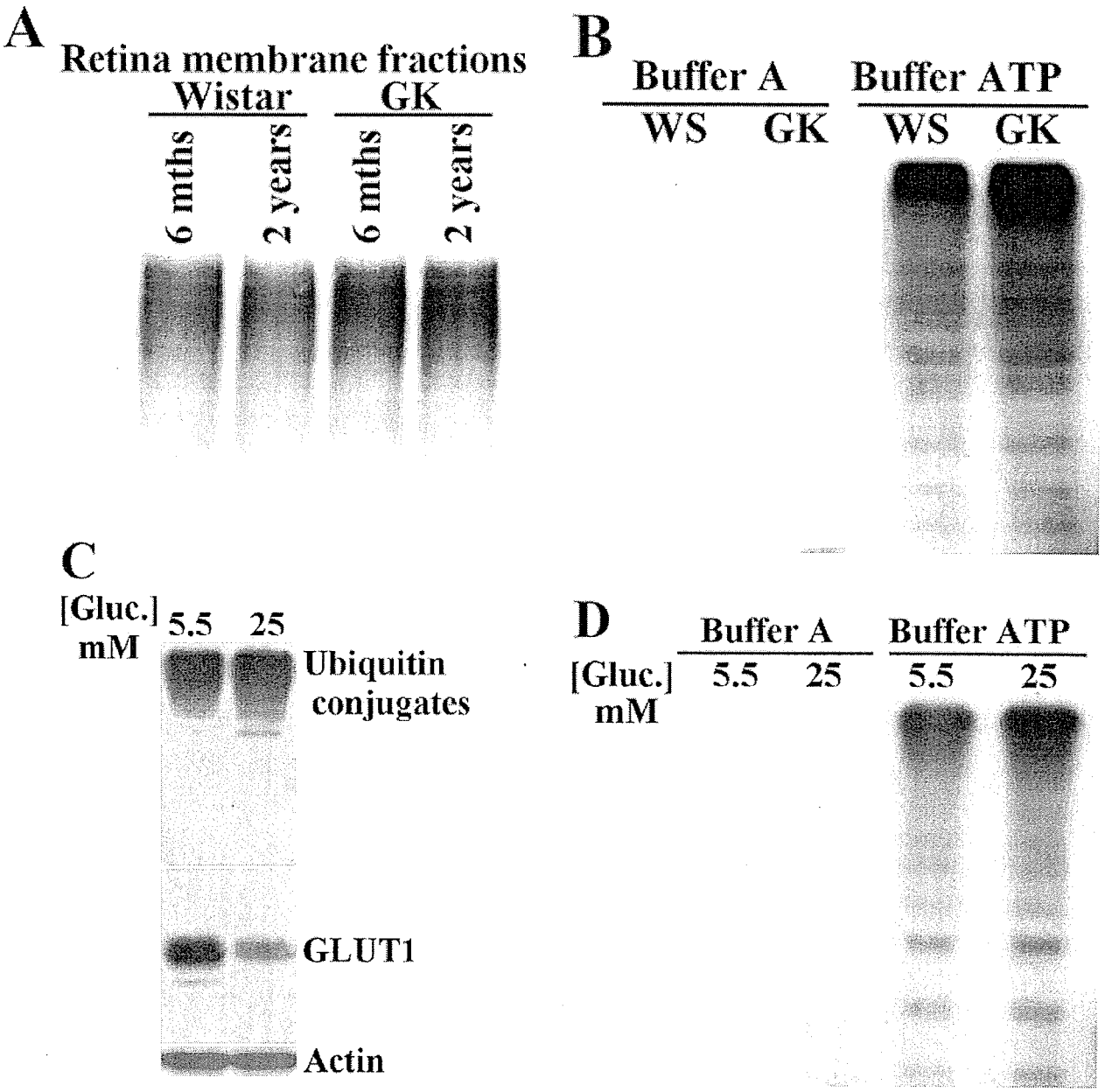


Figure 4. Effect of hyperglycemia on ubiquitinylation. Hyperglycemia altered endogenous ubiquitin conjugates and de novo ubiquitin conjugation activity in diabetic animal (**A**, **B**) and in cells exposed to high glucose (**C**, **D**). Diabetic animals (**A**, lanes labeled "GK") or cells exposed to high glucose (**C**, right) show increased levels of endogenous high molecular weight ubiquitin conjugates. Cells exposed to high glucose also show a significant decrease in the total amount of GLUT1 (**C**). Retinal tissues or cells were lysed, proteins were separated by SDS-PAGE, transferred to PVDF membranes and probed with antibodies directed against ubiquitin conjugates (FK2). The increase in endogenous ubiquitin conjugates is associated with an increased ability of retinal (**B**) or cell (**D**) extracts to conjugate radiolabeled $^{125}$I-ubiquitin to endogenous substrates. Conjugation activity was determined either in the presence of an ATP generating buffer ("Buffer ATP" in **B** and **D**) or as a control in the absence of ATP ("Buffer A" in **B** and **D**). Conjugation experiments were performed for 20 min. Proteins were resolved by SDS-PAGE and the dried gels were used for autoradiography.

The average blood glucose concentrations and body weight for the 6 months and 1 year old diabetic GK rats and age matched Wistar rats are provided in Table 1. Data on diabetic rabbits and healthy controls are provided in Table 2. Diabetic rats were hyperglycemic and they failed to gain weight at a normal rate. The average blood glucose concentrations for diabetic rats and rabbits was significantly higher ($p<0.01$) than that of control animals.

For this study, two retinal endothelial cell models were used. A first approach to the effect of hyperglycemia on GLUT1 levels used primary cultures of endothelial cells obtained from bovine retinas. Once glucose-related changes were established in primary cultures, a cell line was used. TR-iBRB is a conditionally immortalized retinal capillary endothelial cell line. The cells present a doubling time of 19-21 h and exhibit the properties of retinal capillary endothelial cells [7]. To mimic the diabetic condition, both cell types were exposed to high glucose.

*Diabetic animals present lower levels of GLUT1 in retina:* To study the effect of chronic hyperglycemia on GLUT1 expression, we analysed the GLUT1 content in membrane fractions isolated from the whole retinas of diabetic and control animals (Figure 1). As a loading control, membranes were probed with anti-actin antibody. At the age of 6 weeks before GK rats developed diabetes, the Wistar and GK rats showed comparable levels of GLUT1 and endogenous ubiquitin conjugates, thus indicating that the results obtained for older animals are not due to differences in the genetic background of these animals (data not shown). Data presented in Figure 1A indicate that there are no significant changes on GLUT1 protein levels between 6 months old WS rats (2.1±0.40) and GK rats (2.2±0.30). For both control and diabetic rats, an age related decrease on the content of GLUT1 protein was observed. However, GLUT1 expression was significantly lower in of 1 year old GK rats (1.2±0.33) as compared to the age matched WS rats (1.7±0.28), $p<0.05$ level (Figure 1A).

A similar situation is observed in alloxan-induced diabetic rabbits. GLUT1 protein in the retina of non-diabetic rabbits is greater than that in diabetic rabbits (Figure 1B). Since no age-related changes were observed in normal rabbits (data not shown), only one time point was considered in Figure 1B for control animals. To confirm that equal amounts of protein were loaded on each lane, the membranes were stripped and reprobed for actin. Diabetic animals with a duration of disease of 4 months presented a 50% decrease on the amount of the glucose transporter in the retina (control rabbits: 5.7±0.50 and diabetic rabbits: 2.7±0.25; $p<0.01$).

The levels of GLUT1 mRNA were determined by RT-PCR. Total RNA was isolated from whole retinas from rabbits and rats and GLUT1 was amplified by RT-PCR (Figure 1C). β-actin was amplified to confirm that equal quantities of RNA were used for the amplification. There is no evidence for a decrease on mRNA for GLUT1; therefore, the lower levels of protein are probably the result of an increased degradation of GLUT1 associated with diabetes.

*High glucose results in a decrease in GLUT1 in retinal endothelial cells:* As a first approach to study GLUT1 expression upon hyperglycemia, we used primary retinal endothelial cells in culture. BREC were incubated in the presence of low (5.5 mM) and high (25 mM) glucose up to 48 h and cells were then lysed and protein separated by SDS-PAGE, transferred to PVDF membranes and probed with antibodies against GLUT1 (Figure 2). After 48 h of incubation with high glucose, there is a decrease of approximately 35% in the

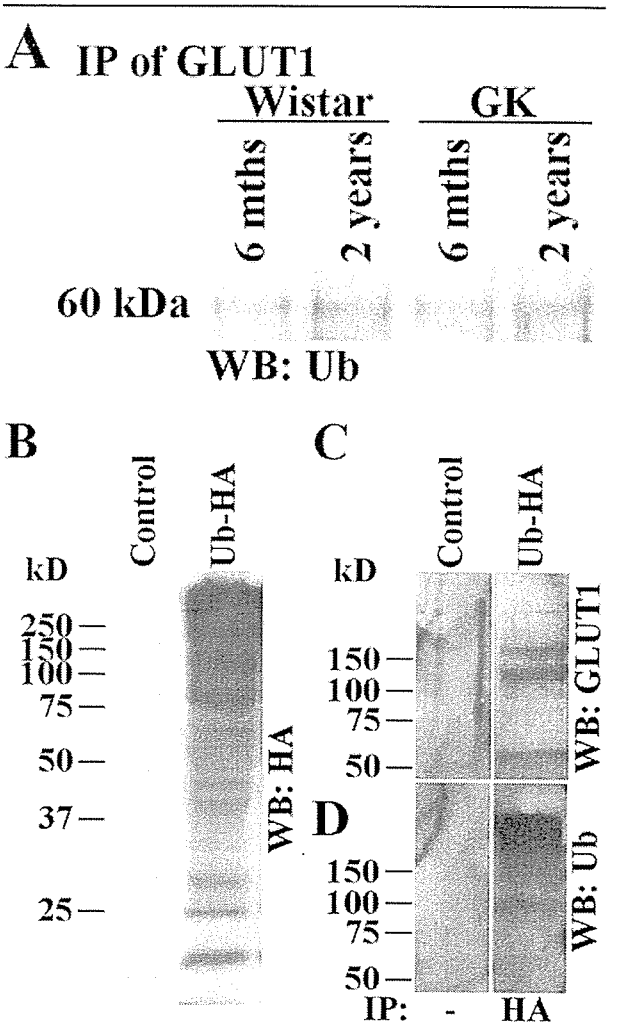


Figure 5. Evidence for ubiquitinylation of GLUT1 in vivo. **A**: GLUT1 was immunoprecipitated from retinal lysates obtained from Wistar (control) and GK (diabetic) rats. Proteins were resolved by SDS-PAGE, transferred to PVDF membranes, and probed with antibodies directed against ubiquitin conjugates (FK2). The additional band with molecular weight around 60 kDa is compatible with a monoubiquitinylated form of GLUT1. **B**: HEK cells were transfected with multiubiquitin tagged to HA (Ub-HA). The cells were lysed and their proteins were resolved by SDS-PAGE, transferred to PVDF membranes, and probed with antibodies directed against HA. This showed efficient transfection and formation of endogenous Ub-HA conjugates had occurred. **C**: Immunoprecipitates of Ub-HA conjugates were subsequently probed with antibodies directed against GLUT1. **D**: Samples were immunoprecipitated with anti-HA and probed with antibodies directed against ubiquitin conjugates.

GLUT1 content as compared to control cells. This observation is consistent with the putative increase in GLUT1 degradation observed in animal models of diabetes.

Considering the practical limitations associated with the use of primary cultures of retina endothelial cells, we chose to use the TR-iBRB, which have been described as a good model for endothelial cells of inner blood-retinal barrier [7]. To investigate whether TR-iBRB would show a similar glucose-dependent decrease of GLUT1, cells were incubated either in the presence of 5.5 mM or 25 mM (hyperglycemia) glucose.

The proteins from TR-iBRB cells were separated by SDS-PAGE, transferred to PVDF membranes and probed with antibodies against GLUT1 (Figure 3A). The data are presented as percentage of the control after 1 h of incubation. After 48 h of incubation, cells treated with high glucose showed a significant decrease ($p<0.05$) in the content of GLUT1 (90.6±7.08%) as compared to control cells (165±8.38%).

The expression of GLUT1 mRNA in high glucose treated TR-iBRB cells was evaluated by northern blotting. The data presented in Figure 3B show the amount of mRNA as percentage of controls after 1 h of incubation. There is no significant change in the levels of GLUT1 mRNA between the cells incubated in medium containing high and low glucose.

*Diabetes is associated with increased ubiquitinylation of retinal proteins:* The levels of GLUT1 of diabetic animals are lower compared to control animals (Figure 1A,B) and incubation of cultured endothelial cells in hyperglycemic conditions leads to a decrease on the GLUT1 expression (Figure 2, Figure 3A). However, in none of the tested conditions was there a significant change in the levels of mRNA for GLUT1 (Figure 1C, Figure 3B). These data led us to hypothesize that the stability of GLUT1 is decreased in diabetes or under hyperglycemia. Since the ubiquitin conjugating system is one of the proteolytic systems involved in regulating protein stability [18,19], we looked for evidence of increased ubiquitinylation in retinas of diabetic animals.

Membrane protein fractions from 6 months and 2 years old GK and WS rats were separated by SDS-PAGE, transferred to PVDF membranes and probed with antibodies directed against ubiquitin. The ubiquitinylated high molecular weight conjugates were more abundant in the GK rats than in age matched WS rats (Figure 4A). When TR-iBRB cells were exposed to hyperglycemia for 15 days, a slight increase on the total amount of endogenous high molecular weight ubiquitin conjugates was observed, compared to those observed in euglycemic conditions, with a paralleled decrease in the GLUT1 content (Figure 4C), consistent with what was observed for the animal models of diabetes (Figure 4A). The endogenous ubiquitin conjugates were analysed after 15 days of high glucose treatment since only at this time point a significant increase in endogenous ubiquitin conjugates could be observed whereas GLUT1 content decreases after 48 h of incubation with high glucose (Figure 3A).

*Conjugation of ubiquitin to GLUT1 is associated with increased degradation of the protein in endothelial cells:* Since data show that diabetes is associated with an increase on the amount of ubiquitin-protein conjugates in the retina of rats and in TR-iBRB cells exposed to high glucose, we further investigated whether such an increase on ubiquitin-protein conjugates is associated with an increase in the ability of retinal endothelial cell lysates to conjugate exogenous ubiquitin to endogenous substrates. Ubiquitin conjugating activity was evaluated as the ability of retinal lysates to conjugate exogenous radiolabeled ubiquitin ($^{125}$I-Ub) to endogenous substrates. Data presented in Figure 4B show that retinal lysates from diabetic animals present an increase of about 45% in the ability to conjugate exogenous ubiquitin to endogenous substrates. This increase in conjugation activity is reflected by the accumulation of high molecular weight ubiquitinylated proteins in retinas from diabetic animals (Figure 4B). The formation of protein-ubiquitin conjugates is ATP-dependent, since there are not any conjugates formed in the absence of ATP (Figure 4B, compare "Buffer A" with "Buffer ATP").

We further evaluated the ubiquitin conjugating activity in the TR-iBRB cells exposed to high glucose. Consistent to what was observed for retinas of diabetic animals, the cytosolic fractions from TR-iBRB cells treated with high glucose concentrations showed a higher ability (approximately 28%) to form de novo ubiquitin conjugates as compared to cells treated in euglycemic concentrations (Figure 4D).

Since the proteasome is inhibited during the conjugation assays, the above data further suggest that the increase in endogenous ubiquitin conjugates in hyperglycemic conditions (GK rats and TR-iBRB cells treated with high glucose) is most likely associated with an increase on the amount of substrates prone to ubiquitinylation or an up-regulation of the activity and/or conjugating enzymes.

To investigate a possible association between GLUT1 and ubiquitin, the retinal membrane extracts from GK and WS rats were used to immunoprecipitate (IP) GLUT1. Immunoprecipitated proteins were separated by SDS-PAGE, transferred to PVDF and probed with antibodies directed against ubiquitin. A band of molecular weight near 60 kDa was detected. Because ubiquitin has a molecular mass of 8.6 kDa, this 60 kDa protein is likely to correspond to a monoubiquitinylated form of GLUT1 since its molecular weight is consistent with the addition of one ubiquitin molecule to GLUT1. Interestingly, this band is more intense in the 2 year old animals (GK and WS rats) than in the 6 month old rats (Figure 5A). This probably indicates that GLUT1 is ubiquitinylated in an age-dependent way and that diabetes creates the conditions that further lead to an enhanced conjugation of ubiquitin to GLUT1. To further investigate the hypothesis that GLUT1 is ubiquitinylated in vivo, we transfected HEK293 cells with a HA-tagged ubiquitin cDNA, and the cell lysates were analysed to confirm efficient ubiquitinylation of cell proteins with HA-tagged ubiquitin (Figure 5B). The extracts were also used to immunoprecipitate protein-ubiquitin conjugates with an antibody against the HA epitope. Proteins were resolved by SDS-PAGE, transferred to PVDF, and the membrane was probed with antibodies against GLUT1 (Figure 5C) or against ubiquitin (Figure 5D). The immunoblot analysis showed that GLUT1 is co-precipitated with ubiquitin-HA (Figure 5C). The high molecular weight bands that cross reacted with the anti-

GLUT1 antibody are likely to correspond to ubiquitinylated GLUT1. A band of approximately 50 kDa, attributed to unmodified GLUT1, is also present in the HA-ubiquitin immunoprecipitates. The presence of this band in HA immunoprecitates may indicate that GLUT1 interacts in vivo with a protein that is involved in the ubiquitin proteasome pathway and that is most likely ubiquitinylated in vivo.

## DISCUSSION

The regulation of GLUT1 levels in retinal endothelial cells subjected to chronic hyperglycemia remains a matter of controversy, since there are conflicting reports in the literature [4,6,20].

In this study, we used two different animal models of diabetes, as well as a primary culture of endothelial cells and a cell line that expresses GLUT1. To mimic hyperglycemia endothelial cells were exposed to high glucose, in order to clarify the effect of diabetes on the level of expression of GLUT1. We showed that the amount of GLUT1 present in membrane fractions isolated from whole retinas of diabetic rats or rabbits is subnormal. Our data are in agreement with the results reported by Tang et al [21], showing a decrease in GLUT1 expression in retinal vascular endothelium (55%) and in homogenates of whole retina (36%) of streptozotocin-induced diabetic rats. Consistently, the results of Badr et al. showed that streptozotocin-induced diabetes reduced GLUT1 expression in the retina and its microvasculature by approximately 50% [4]. However, ultrastructural localization of GLUT1 showed increased expression of GLUT1 transporter in retinal capillaries of three diabetic patients [20]. Apparently, such contradictory observations could be due to the different approaches used to quantify GLUT1. In fact, as shown by the present data, other studies in whole retinal vasculature homogenates suggest a decrease in GLUT1 expression caused by diabetes in several different diabetic models [4,21]. On the other hand, ultrastructural localization of GLUT1 and quantification of GLUT1 sites at the capillary membranes detected either increased GLUT1 levels [20] or no changes in GLUT1 levels [22] in diabetes. Taken together, these observations suggest that the decrease on total pool of GLUT1 caused by diabetes (reported by Badr et al [4] and the present data) may not limit GLUT1 targeting to plasma membranes but may result in a reduction on the available pool of intracellular GLUT1 that could eventually compromise efficient recycling of the transporter.

The observation that hyperglycemic conditions induce a significant decrease on the amount of GLUT1 protein without significant changes on the levels of its mRNA led us to hypothesize that such decreased levels of GLUT1 may result from an increase on the degradation rate of the protein. Alterations in protein turnover during diabetes have been previously correlated with increased activity of the ubiquitin-dependent proteolytic system in skeletal [23,24] and cardiac [25] muscle. Moreover, the severity of electroneurographic changes in patients with *type 2* diabetes has been correlated with increased serum ubiquitin levels [26]. Our results show that both retinal extracts from GK rats and TR-iBRB cells treated with high glucose present increased levels of ubiquitin conjugates as compared to controls (Figure 4A,C). The increase in the endogenous ubiquitin conjugates seems to be associated with an increased ubiquitin conjugating activity as revealed by the increased ability of tissue or cell extracts to conjugate exogenous ubiquitin to endogenous substrates (Figure 4B,D). This suggests that, in agreement to what has been observed for other tissues particularly affected by diabetes, there is an accumulation of ubiquitin conjugates and an increase in the ubiquitin conjugating activity in the retina during diabetes. Importantly these alterations can be mimicked by exposing primary culture of endothelial cells or a retinal endothelial cell line to high concentrations of glucose. The use of primary cultures of retinal endothelial cells further showed that GLUT1 in endothelial cells responds to high glucose in a manner similar to that observed for entire retinas of diabetic animals.

Since our data suggest increased degradation of GLUT1 during diabetes (Figure 1, Figure 2, and Figure 3) and since we observed an increase on ubiquitin conjugates in hyperglycemic conditions, we tested whether ubiquitinylation is the mechanism targeting GLUT1 degradation.

GLUT1 immunoprecipitated from membrane protein fractions of control and diabetic rats cross-reacts with antibodies to ubiquitin on western blots. This suggests that a ubiquitin-like modification occurs in GLUT1, particularly in the older (control and diabetic) animals. A more detailed evaluation of the role of ubiquitinylation on targeting GLUT1 for degradation was performed in TR-iBRB cells.

The immunoprecipitates of ubiquitin-protein conjugates from cells overexpressing hemagglutinin-tagged ubiquitin also revealed crossreactivity with antibodies directed against GLUT1. The presence in the HA-ubiquitin immunoprecipitates of several bands that crossreact with anti-GLUT1 antibody could be due to the uncomplete processing of the construct of multiubiquitins in the transfected cells. This approach showed that GLUT1 is ubiquitinylated, but it does not allow us to ascertain whether it is mono or polyubiquitinylated. We suggest that ubiquitin is the triggering signal that targets the glucose transporter GLUT1 for degradation either by lysosomes or proteasomes.

The ubiquitin proteasome pathway is involved in virtually all aspects of cell regulation [27]. The ubiquitin-dependent proteolytic pathway involves covalent conjugation of ubiquitin to substrates in a process dependent on ATP. Whereas it has been clearly established that, in most cases, conjugation of a protein to ubiquitin results in its degradation by the 26S proteasome, it has more recently been suggested that monoubiquininylation is associated with lysosomal degradation of targeted proteins [28,29].

More recently, several proteins have been identified as being highly homologous to ubiquitin. Sentrin (or SUMO-1) is a small ubiquitin-like protein [30]. To date only six main substrates for sentrin have been characterized in mammalian cells. Whereas it has been clearly established that in most cases conjugation of a protein to ubiquitin results in its degradation by the proteasome, it has more recently been suggested that conjugation of sentrin to protein substrates, through Ubc9, is

associated with changes in its subcellular distribution [31]. Recently it was shown that both GLUT1 and GLUT4 are modified by sentrin in skeletal muscle cells and that the specialized conjugating enzyme, Ubc9, differentially regulates the cellular levels of the two GLUTs [32]. Overexpression of mUbc9 in these cells resulted in a decrease in GLUT1 abundance, presumably by targeting the protein for degradation.

We show that GLUT1 is ubiquitinylated in the retina and in endothelial cells and that aging and, significantly, diabetes are associated with an increased ubiquitinylation of GLUT1. By analogy to several other membrane proteins we can suggest that GLUT1 is most likely monoubiquitinylated and presumably degraded by lysosomes.

In conclusion, ubiquitinylation plays a role in the regulation of GLUT1 levels in endothelial cells in hyperglycemia and may ultimately constitute a novel level of regulation through which glucose transport into endothelial cells may transduce pathophysiological changes associated with diabetic retinopathy.

## ACKNOWLEDGEMENTS

We thank Professor João Patrício and coworkers (Laboratory Animals Research Center, University Hospital, Coimbra, Portugal) for maintaining the animals.

RF was the recipient of a Fellowship from Foundation for Science and Technology, Portugal (PRAXIS XXI/BD/15583/98). This work was also supported by grants from Luso-American Foundation for Development and Portuguese Foundation for Science and Technology (FCT; Programme POCTI).

## REFERENCES

1. King GL, Kunisaki M, Nishio Y, Inoguchi T, Shiba T, Xia P. Biochemical and molecular mechanisms in the development of diabetic vascular complications. Diabetes 1996; 45:S105-8.
2. Lorenzi M. Glucose toxicity in the vascular complications of diabetes: the cellular perspective. Diabetes Metab Rev 1992; 8:85-103.
3. Kumagai AK, Glasgow BJ, Pardridge WM. GLUT1 glucose transporter expression in the diabetic and nondiabetic human eye. Invest Ophthalmol Vis Sci 1994; 35:2887-94.
4. Badr GA, Tang J, Ismail-Beigi F, Kern TS. Diabetes downregulates GLUT1 expression in the retina and its microvessels but not in the cerebral cortex or its microvessels. Diabetes 2000; 49:1016-21.
5. Mandarino LJ, Finlayson J, Hassell JR. High glucose downregulates glucose transport activity in retinal capillary pericytes but not endothelial cells. Invest Ophthalmol Vis Sci 1994; 35:964-72.
6. Busik JV, Olson LK, Grant MB, Henry DN. Glucose-induced activation of glucose uptake in cells from the inner and outer blood-retinal barrier. Invest Ophthalmol Vis Sci 2002; 43:2356-63.
7. Hosoya K, Tomi M, Ohtsuki S, Takanaga H, Ueda M, Yanai N, Obinata M, Terasaki T. Conditionally immortalized retinal capillary endothelial cell lines (TR-iBRB) expressing differentiated endothelial cell functions derived from a transgenic rat. Exp Eye Res 2001; 72:163-72.
8. Hershko A, Ciechanover A, Heller H, Haas AL, Rose IA. Proposed role of ATP in protein breakdown: conjugation of protein with multiple chains of the polypeptide of ATP-dependent proteolysis. Proc Natl Acad Sci U S A 1980; 77:1783-6.
9. Kumagai AK, Kang YS, Boado RJ, Pardridge WM. Upregulation of blood-brain barrier GLUT1 glucose transporter protein and mRNA in experimental chronic hypoglycemia. Diabetes 1995; 44:1399-404.
10. Boado RJ, Pardridge WM. The brain-type glucose transporter mRNA is specifically expressed at the blood-brain barrier. Biochem Biophys Res Commun 1990; 166:174-9.
11. Goto Y, Suzuki K, Ono T, Sasaki M, Toyota T. Development of diabetes in the non-obese NIDDM rat (GK rat). Adv Exp Med Biol 1988; 246:29-31.
12. Agardh CD, Agardh E, Zhang H, Ostenson CG. Altered endothelial/pericyte ratio in Goto-Kakizaki rat retina. J Diabetes Complications 1997; 11:158-62.
13. Miyamoto K, Ogura Y, Nishiwaki H, Matsuda N, Honda Y, Kato S, Ishida H, Seino Y. Evaluation of retinal microcirculatory alterations in the Goto-Kakizaki rat. A spontaneous model of non-insulin-dependent diabetes. Invest Ophthalmol Vis Sci 1996; 37:898-905.
14. Sone H, Kawakami Y, Okuda Y, Sekine Y, Honmura S, Matsuo K, Segawa T, Suzuki H, Yamashita K. Ocular vascular endothelial growth factor levels in diabetic rats are elevated before observable retinal proliferative changes. Diabetologia 1997; 40:726-30.
15. Goto Y, Kakizaki M, Masaki N. Spontaneous diabetes produced by selective breeding of normal wistar rats. Proc Jpn Acad 1975; 51:80-5.
16. Engerman RL, Bloodworth JM Jr. Experimental diabetic retinopathy in dogs. Arch Ophthalmol 1965; 73:205-10.
17. Vinores SA, Derevjanik NL, Mahlow J, Berkowitz BA, Wilson CA. Electron microscopic evidence for the mechanism of blood-retinal barrier breakdown in diabetic rabbits: comparison with magnetic resonance imaging. Pathol Res Pract 1998; 194:497-505.
18. Horak J. The role of ubiquitin in down-regulation and intracellular sorting of membrane proteins: insights from yeast. Biochim Biophys Acta 2003; 1614:139-55.
19. Desterro JM, Rodriguez MS, Hay RT. Regulation of transcription factors by protein degradation. Cell Mol Life Sci 2000; 57:1207-19.
20. Kumagai AK, Vinores SA, Pardridge WM. Pathological upregulation of inner blood-retinal barrier Glut1 glucose transporter expression in diabetes mellitus. Brain Res 1996; 706:313-7.
21. Tang J, Zhu XW, Lust WD, Kern TS. Retina accumulates more glucose than does the embryologically similar cerebral cortex in diabetic rats. Diabetologia 2000; 43:1417-23.
22. Fernandes R, Suzuki K, Kumagai AK. Inner blood-retinal barrier GLUT1 in long-term diabetic rats: an immunogold electron microscopic study. Invest Ophthalmol Vis Sci 2003; 44:3150-4.
23. Rodriguez T, Busquets S, Alvarez B, Carb N, Agell N, Lpez-Soriano FJ, Argils JM. Protein turnover in skeletal muscle of the diabetic rat: activation of ubiquitin-dependent proteolysis. Int J Mol Med 1998; 1:971-7.
24. Galban VD, Evangelista EA, Migliorini RH, do Carmo Kettelhut I. Role of ubiquitin-proteasome-dependent proteolytic process in degradation of muscle protein from diabetic rabbits. Mol Cell Biochem 2001; 225:35-41.
25. Liu Z, Miers WR, Wei L, Barrett EJ. The ubiquitin-proteasome proteolytic pathway in heart vs skeletal muscle: effects of acute diabetes. Biochem Biophys Res Commun 2000; 276:1255-60.
26. Akarsu E, Pirim I, Capoglu I, Deniz O, Akcay G, Unuvar N. Relationship between electroneurographic changes and serum ubiquitin levels in patients with type 2 diabetes. Diabetes Care

2001; 24:100-3.
27. Kornitzer D, Ciechanover A. Modes of regulation of ubiquitin-mediated protein degradation. J Cell Physiol 2000; 182:1-11.
28. Hicke L. A new ticket for entry into budding vesicles-ubiquitin. Cell 2001; 106:527-30.
29. Hicke L, Dunn R. Regulation of membrane protein transport by ubiquitin and ubiquitin-binding proteins. Annu Rev Cell Dev Biol 2003; 19:141-72.
30. Matunis MJ, Coutavas E, Blobel G. A novel ubiquitin-like modification modulates the partitioning of the Ran-GTPase-activating protein RanGAP1 between the cytosol and the nuclear pore complex. J Cell Biol 1996; 135:1457-70.
31. Matunis MJ, Wu J, Blobel G. SUMO-1 modification and its role in targeting the Ran GTPase-activating protein, RanGAP1, to the nuclear pore complex. J Cell Biol 1998; 140:499-509.
32. Giorgino F, de Robertis O, Laviola L, Montrone C, Perrini S, McCowen KC, Smith RJ. The sentrin-conjugating enzyme mUbc9 interacts with GLUT4 and GLUT1 glucose transporters and regulates transporter levels in skeletal muscle cells. Proc Natl Acad Sci U S A 2000; 97:1125-30.

The print version of this article was created on 30 Aug 2004. This reflects all typographical corrections and errata to the article through that date. Details of any changes may be found in the online version of the article.

*Journal of Neurochemistry*, 2004, **89**, 503–513 doi:10.1111/j.1471-4159.2004.02343.x

# A pericyte-derived angiopoietin-1 multimeric complex induces occludin gene expression in brain capillary endothelial cells through Tie-2 activation *in vitro*

Satoko Hori,*,†,¶ Sumio Ohtsuki,*,†,¶ Ken-ichi Hosoya,‡,¶ Emi Nakashima§,¶ and Tetsuya Terasaki*,†,¶

**Department of Molecular Biopharmacy and Genetics, Graduate School of Pharmaceutical Sciences, Tohoku University, Aoba-ku, Sendai, Japan*

*†New Industry Creation Hatchery Center, Tohoku University, Aoba-ku, Sendai, Japan*

*‡Faculty of Pharmaceutical Sciences, Toyama Medical and Pharmaceutical University, Toyama, Japan*

*§Department of Pharmaceutics, Kyoritsu College of Pharmacy, Minato-ku, Tokyo, Japan*

*¶CREST and SORST of the Japan Science and Technology Agency (JST), Japan*

**Abstract**

Although tight-junctions (TJs) at the blood–brain barrier (BBB) are important to prevent non-specific entry of compounds into the CNS, molecular mechanisms regulating TJ maintenance remain still unclear. The purpose of this study was therefore to identify molecules, which regulate occludin expression, derived from astrocytes and pericytes that ensheathe brain microvessels by using conditionally immortalized adult rat brain capillary endothelial (TR-BBB13), type II astrocyte (TR-AST4) and brain pericyte (TR-PCT1) cell lines. Transfilter co-culture with TR-AST4 cells, and exposure to conditioned medium of TR-AST4 cells (AST-CM) or TR-PCT1 cells (PCT-CM) increased occludin mRNA in TR-BBB13 cells. PCT-CM-induced occludin up-regulation was significantly inhibited by an angiopoietin-1-neutralizing antibody, whereas the up-regulation by AST-CM was not. Immunoprecipitation and western blot analyses confirmed that multimeric angiopoietin-1 is secreted from TR-PCT1 cells, and induces occludin mRNA, acting through tyrosine phosphorylation of Tie-2 in TR-BBB13 cells. A fractionated AST-CM study revealed that factors in the molecular weight range of 30–100 kDa led to occludin induction. Conversely, occludin mRNA was reduced by transforming growth factor β1, the mRNA of which was up-regulated in TR-AST4 cells following hypoxic treatment. In conclusion, *in vitro* BBB model studies revealed that the pericyte-derived multimeric angiopoietin-1/Tie-2 pathway induces occludin expression.

**Keywords:** astrocyte, blood–brain barrier, multimeric angiopoietin-1, occludin, pericyte, Tie-2.

*J. Neurochem.* (2004) **89**, 503–513.

Tight-junctions (TJs) form barriers between adjacent brain capillary endothelial cells (BCECs) at the blood–brain barrier (BBB) and play an important role in preventing non-specific paracellular transport in order to protect the CNS. Brain disorders, such as brain tumors, infarcts and encephalitis, cause TJ disruption to allow BBB leakage (Davies 2002). Therefore, clarifying the mechanism of TJ maintenance is important for understanding and treating CNS diseases associated with BBB leakage.

BCECs are surrounded by pericytes and astrocyte foot processes. The overall brain microvascular biology is a function of the paracrine interactions between BCECs and the two other types of cells (Pardridge 1999; Gaillard

Received August 22, 2003; revised manuscript received November 24, 2003; accepted December 31, 2003.

Address correspondence and reprint requests to Professor Tetsuya Terasaki, Department of Molecular Biopharmacy and Genetics, Graduate School of Pharmaceutical Sciences, Tohoku University, Aoba, Aramaki, Aoba-ku, Sendai 980–8578, Japan.

E-mail: terasaki@mail.pharm.tohoku.ac.jp

*Abbreviations used*: AST (PCT)-CM, conditioned medium of TR-AST (TR-PCT) cells; BBB, blood–brain barrier; BCEC, brain capillary endothelial cell; CM, conditioned medium; ECGF, endothelial cell growth factor; JAM, junctional adhesion molecule; PI3-kinase, phosphatidylinositol 3-kinase; PTyr, phosphotyrosine; TEER, transendothelial electrical resistance; TGF-β1, transforming growth factor β1; TJ, tight-junction; TR-AST, conditionally immortalized rat astrocyte cell line; TR-BBB, conditionally immortalized rat brain capillary endothelial cell line; TR-PCT, conditionally immortalized rat pericyte cell line; VEGF, vascular endothelial growth factor.

 

*et al.* 2000; Abbott 2002). Astrocytes are known to induce TJs of non-CNS endothelial cells *in vivo* (Janzer and Raff 1987). As for brain pericytes, their recruitment and association with microvessels are also key processes in normal vascular development and maintenance. It has been shown that platelet-derived growth factor-B knock-out mice lack brain pericytes, and die due to hemorrhage (Lindahl *et al.* 1997). Therefore, it is conceivable that paracrine interactions between BCECs, and astrocytes and pericytes, play important roles in maintaining TJs at the BBB.

Occludin (Furuse *et al.* 1993; Hirase *et al.* 1997), which is a transmembrane protein, is exclusively localized at the TJ strands of the BBB, together with junctional adhesion molecule (JAM) (Martin-Padura *et al.* 1998), claudin-5 and claudin-12 (Nitta *et al.* 2003). These transmembrane proteins are important in regulating the paracellular permeability by interacting with each other in both a homophilic and heterophilic manner between adjacent cells, and by becoming linked to the cytoskelton through a complex of accessory proteins such as ZO-1/ZO-2/ZO-3. Since occludin expression is down-regulated in various brain disorders accompanied by TJ disruption (Huber *et al.* 2001; Davies 2002), the expression level of occludin is important for TJ maintenance at the mature BBB. Therefore, identifying physiological occludin-regulators will provide deeper insight into the maintenance and recovery of the TJ properties at the BBB.

Angiopoietin-1, a ligand of tyrosine kinase Tie-2, is known to be an anti-permeability factor in the peripheral vascular system (Davis *et al.* 1996). It has recently been reported that administration of angiopoietin-1 reduces BBB leakage in the ischemic brain (Zhang *et al.* 2002), suggesting that angiopoietin-1 has an anti-permeability effect on the BBB as well as the peripheral vascular system. In contrast, transforming growth factor β1 (TGF-β1) and vascular endothelial growth factor (VEGF) are vascular permeability factors, and have been reported to be increased in the brain in various neurodegenerative diseases (Kalaria *et al.* 1998; Lesne *et al.* 2002). We hypothesize that these soluble factors are secreted from astrocytes and/or brain pericytes in the mature CNS, and involved in TJ regulation at the BBB under physiological and pathophysiological conditions.

Induction and maintenance of the TJ properties at the BBB depend critically on the local conditions and maturational state. In the present study, in order to clarify the astrocyte- and pericyte-derived factors involved in TJ maintenance, we selected conditionally immortalized brain endothelial (TR-BBB) (Hosoya *et al.* 2000b), type II astrocyte (TR-AST) (Tetsuka *et al.* 2001), and brain pericyte (TR-PCT) (Asashima *et al.* 2002; Asashima *et al.* 2003) cell lines, which had been established from adult transgenic rats harboring temperature-sensitive simian virus 40 large T-antigen (Obinata 1997; Takahashi *et al.* 1999) and which retain their *in vivo* function well (Terasaki and Hosoya 2001; Terasaki *et al.* 2003).

The purpose of the present study was to clarify the mechanism of occludin induction and identify occludin-inducing molecules by using conditionally immortalized BBB cell lines, which are of the same maturational stage, strain, and genetic background. The change in occludin expression level was quantified in TR-BBB13 cells during transfilter co-culture with TR-AST4 cells and on treatment with the conditioned medium of TR-AST4 cells (AST-CM) or TR-PCT1 cells (PCT-CM). We also investigated the effect of angiopoietin-1 in conditioned medium, TGF-β1 and VEGF on occludin expression, and Tie-2 activation by PCT-CM to clarify the signal pathway for occludin regulation.

## Materials and methods

### Animals

Male Wistar rats, weighing 250–300 g, were purchased from Charles River (Yokohama, Japan). The investigations using rats described in this report conformed to the guidelines established by the Animal Care Committee, Graduate School of Pharmaceutical Sciences, Tohoku University.

### Reagents

Endothelial cell growth factor (ECGF) was purchased from Boehringer Mannheim (Mannheim, Germany); benzylpenicillin potassium and streptomycin sulfate were purchased from Wako Pure Chemical Industries (Osaka, Japan); recombinant human angiopoietin-1 was purchased from Genzyme Techne (Minneapolis, MN, USA); recombinant human VEGF and TGF-β1 were purchased from Peprotech EC (London, UK). All other chemicals were commercial products of analytical grade.

### Cell cultures

TR-BBB13, TR-AST4 and TR-PCT1 cells were conditionally immortalized BCEC, astrocyte and pericyte cell lines, respectively (Hosoya *et al.* 2000b; Tetsuka *et al.* 2001; Asashima *et al.* 2002) and used as *in vitro* BBB model (Terasaki *et al.* 2003). TR-BBB13 cells were grown in Dulbecco's modified Eagle's medium (DMEM, Nissui Pharmaceutical, Tokyo, Japan) supplemented with 20 mM sodium bicarbonate, 15 ng/mL ECGF, 100 U/mL benzylpenicillin potassium, 100 μg/mL streptomycin sulfate and 10% fetal bovine serum (Moregate, Bulimba, Australia) (culture medium-A). The culture medium-B for TR-AST4 cells and TR-PCT1 cells consisted of culture medium-A without ECGF. TR-BBB13 cells and TR-PCT1 cells were seeded onto rat tail collagen type I-coated tissue culture dishes (BD Biosciences, Franklin Lakes, NJ, USA). These cells were maintained at 33°C, which is a permissive temperature at which temperature-sensitive SV40 large T-antigen is activated, in a humidified atmosphere of 95% air and 5% $CO_2$. The experimental culture temperature was also 33°C because a long-term culture needs the cell growth conditions. The cells retain the expression of specific markers at 33°C (Hosoya *et al.* 2000b; Tetsuka *et al.* 2001; Asashima *et al.* 2002).

### Transfilter co-culture of TR-BBB13 cells and TR-AST4 cells

TR-BBB13 cells were cultured with TR-AST4 cells in a transfilter co-culture system. In this system, TR-AST4 cells were seeded [$5 \times 10^4$ cells per insert (4.3 $cm^2$)] on the backside membrane of a collagen type I-coated transfilter, a cell culture insert (pore size: 3.0 μm, BD Biosciences) in culture medium-B. After 24-h culture, the insert was transferred to a 6-well plate and TR-BBB13 cells were seeded ($5 \times 10^4$ cells per insert) on the upper side of the insert. In single culture, TR-BBB13 cells were seeded ($5 \times 10^4$ cells per insert) on the upper side of the insert without TR-AST4 cells on the backside. The cells were cultured at 33°C and the culture medium-B was renewed every other day. After a predetermined time period, transendothelial electrical resistance (TEER) in TR-BBB13 cells was measured using Millicell-ERS equipment (Millipore, Bedford, MA, USA), and after that the cells were collected with a cell scraper.

### Preparation of AST-CM and PCT-CM

TR-AST4 cells or TR-PCT1 cells were cultured in culture medium-B without serum. After 24 h, conditioned medium (CM) was collected, concentrated up to 20-fold in a Centriprep-10 (10-kDa cut-off) (Millipore, Bedford, MA, USA) and stored at −20°C until studied. Control CM was prepared by the same procedure using culture medium-B without serum. The CM was adjusted to an appropriate concentration by diluting the 20-fold concentrated CM with culture medium-B without serum.

### Fractionation of CM using size exclusion membranes

CM was concentrated up to 20-fold using a graded series of molecular weight cut-off filters as follows (Millipore). The CM was concentrated using a Centriplus-100 (100-kDa cut-off). The retentate was kept as the > 100-kDa fraction and the filtrate was sequentially concentrated using a Centriprep-50 (50-kDa cut-off) (to obtain a 50- to 100-kDa fraction), Centriprep-30 (30-kDa cut-off) (30- to 50-kDa fraction) and Centriprep-10 (10- to 30-kDa fraction).

### Treatment with AST-CM, PCT-CM, angiopoietin-1, VEGF or TGF-β1

TR-BBB13 cells were treated with AST-CM, PCT-CM or fractionated AST-CMs for 24 h at 33°C. TR-BBB13 cells were treated with angiopoietin-1 (0, 0.1, 1, 10, 100 and 500 ng/mL), VEGF (0, 0.1, 1 and 10 ng/mL) or TGF-β1 (0, 0.1, 1 and 10 ng/mL) for 24 h at 33°C.

### Hypoxic conditions

Hypoxic conditions were achieved with an anaerobic chamber and BBL GasPak Plus (BD Biosciences), which catalytically reduces the oxygen level to less than 10 p.p.m. within 90 min (Shimizu *et al.* 1996). TR-AST4 cells were cultured for 24 h under these hypoxic conditions.

### Angiopoietin-1 inhibitory study

AST-CM and PCT-CM were pre-treated with 0.625 μg/mL antibody against angiopoietin-1 (Chemicon, Temecula, CA, USA) or normal rabbit IgG (control) for 16 h at 4°C. TR-BBB13 cells were cultured with the angiopoietin-1-neutralized-AST-CM or PCT-CM for 24 h at 33°C.

### RT-PCR analysis

Total RNA was extracted from rat tissues, TR-AST4 cells and TR-PCT1 cells using an RNeasy kit (Qiagen, Tokyo, Japan) according to the manufacturer's protocol. Single-stranded cDNA was made from 1 μg total RNA by RT (ReverTraAce, Toyobo, Osaka, Japan) using oligo dT primer. The sequences of primers were as follows: sense primer 5′-AGGAGACGGAATACAGGGCT-3′ and antisense primer 5′-CCGGGTTGTGTTGGTTGTAG-3′ for TGF-β1 (GenBank Accession Number; NM021578); sense primer 5′-CTCAGTGGCTGCAAAAACTTG-3′ and antisense primer 5′-CAGAATTTCATTTGTCTGTTGGA-3′ for angiopoietin-1 (GenBank Accession Number; AB080023); sense primer 5′-TTTGAGACCTTCAACACCCC-3′ and antisense primer 5′-ATAGCTCTTCTCCAGGGAGG-3′ for β-actin (GenBank Accession Number; NM031144). The PCR was performed using GeneAmp (PCR system 9700, Perkin-Elmer, Norwalk, CT, USA) with TGF-β1, angiopoietin-1 and β-actin specific primers through 30 cycles of denaturation for 30 s at 94°C, annealing for 30 s at 60°C, and synthesis for 1 min at 72°C. The sizes of the expected RT-PCR products of TGF-β1, angiopoietin-1 and β-actin were 416, 275 and 352 bp, respectively. The RT-PCR of each sample RNA without the RT was used as a negative control. The RT-PCR products were separated by electrophoresis on an agarose gel in the presence of ethidium bromide (0.6 μg/mL) and visualized using an imager (EPIPRO 7000; Aisin, Aichi, Japan). The PCR products were subcloned into a plasmid vector using pGEM-T Easy Vector System I (Promega, Madison, WI, USA) and then sequenced from both directions using a DNA sequencer (CEQ2000XL DNA Analysis System; Beckman Coulter, Fullerton, CA, USA). Sequence comparisons were made using the GENETYX software package, version 6.1.0 (Genetyx, Tokyo, Japan).

### Quantitative real-time PCR analysis

Total RNA was extracted from TR-BBB13 cells using an RNeasy kit according to the manufacturer's protocol. RNA integrity was checked by electrophoresis on an agarose gel. Quantitative real-time PCR analysis was performed using an ABI PRISM 7700 sequence detector system (PE Applied Biosystems, Foster City, CA, USA) with 2× SYBR Green PCR Master Mix (PE Applied Biosystems) as per the manufacturer's protocol. To quantify the amount of specific mRNA in the samples, a standard curve was generated for each run using pGEM-T Easy Vector containing occludin, JAM or β-actin (dilution ranging from 0.1 fg/μL to 1 ng/μL). This enabled standardization of the initial mRNA content of TR-BBB13 cells relative to the quantity of β-actin. The control lacking the RT enzyme was assayed in parallel to monitor any possible genomic contamination. PCR was performed through 40 cycles of 95°C for 30 s, 60°C for 1 min, and 72°C for 1 min after pre-incubation at 95°C for 10 min using specific primers. The sequences of primers were as follows: sense primer 5′-GCCTTTTGCTTCATCGCTTCC-3′ and antisense primer 5′-AACAATGATTAAAGCAAAAGCCAC-3′ for occludin (GenBank Accession Number, AB016425); sense primer 5′-ACAGCCATGAGGTCAGAGGCT-3′ and antisense primer 5′-ACCTAGAAGACATTGAAGGCATC-3′ for JAM (GenBank Accession Number, AF276998). The β-actin primers are given above.

### Western blot analysis

The membrane and whole cell lysate fractions of rat brain, isolated rat brain capillary, and TR-BBB13 cells were prepared using the procedure described in a previous report (Hosoya *et al.* 2000a). The AST-CM or PCT-CM was suspended in 10% trichloroacetic acid/acetone, with or without 20 mM dithiothreitol for 1 h at −20°C, followed by centrifugation at 15 000 *g* for 15 min. The pellet was washed with acetone, with or without 20 mM dithiothreitol, then lyzed with lysis buffer (10 mM Tris-HCl pH 7.4, 1% sodium dodecyl sulfate, 1 mM EDTA and 10% glycerol), with or without 5% 2-mercaptoethanol. Protein concentrations were determined by a DC protein assay kit (Bio-Rad, Hercules, CA, USA). Membrane lysate (20 μg per lane) was used for detecting occludin protein in rat tissues and the cell lines (Fig. 1b). Whole cell lysate (50 μg per lane) was used for investigating the effect of the transfilter co-culture on occludin expression (Fig. 1c). Protein samples were electrophoresed on gradient sodium dodecyl sulfate–polyacrylamide gel (Bio-Rad) and subsequently electrotransferred to nitrocellulose membranes. Membranes were treated with blocking buffer (4% skimmed milk in 25 mM Tris-HCl pH 8.0, 125 mM NaCl, 0.1% Tween 20) for 2 h at room temperature and incubated with anti-occludin antibody (0.1 μg/mL; Zymed, San Francisco, CA, USA), anti-β-actin antibody (1 : 2000; Sigma, St.Louis, MO, USA), anti-angiopoietin-1 antibody (1 μg/mL; Santa Cruz Biotechnology, Santa Cruz, CA, USA) or anti-Tie-2 antibody (1 μg/mL; Santa Cruz Biotechnology) for 16 h at 4°C as the primary antibody. The membranes were washed three times with blocking buffer and incubated with horseradish peroxidase-conjugated second antibody. The bands were visualized with an enhanced chemiluminescence kit (SuperSignal; Pierce, Rockford, IL, USA). The relative densities of the bands were measured using NIH image software (National Institutes of Health, Bethesda, MD, USA).

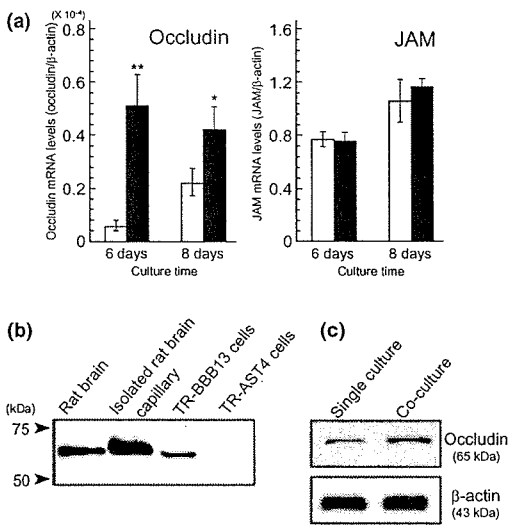


**Fig. 1** Induction of occludin expression in TR-BBB13 cells transfilter co-cultured with TR-AST4 cells. (a) TR-BBB13 cells were transfilter co-cultured with TR-AST4 cells (black column) or single-cultured (open column) for 6 or 8 days. The occludin and JAM mRNA levels were determined by quantitative real-time PCR analysis. Each mRNA expression level was normalized with respect to the β-actin mRNA expression. Each column represents the mean ± SEM ($n = 3$). $^{**}p < 0.01$, $^{*}p < 0.05$, significantly different from the single culture. (b) Western blot analysis of occludin in rat brain and isolated rat brain capillary (positive controls), TR-BBB13 cells and TR-AST4 cells (a negative control). (c) Western blot analysis of occludin (upper) and β-actin (lower) in single-cultured TR-BBB13 cells and TR-BBB13 cells co-cultured with TR-AST4 cells for 8 days. The ratio of occludin to β-actin density in co-culture was 1.77-fold greater than that in single culture ($n = 3$).

### Analysis of tyrosine phosphorylation of Tie-2 protein

TR-BBB13 cells were cultured with two-fold concentrated AST-CM, PCT-CM or 300 ng/mL angiopoietin-1 for 24 h, then collected and suspended in lysis buffer (10 mM Tris-HCl pH 7.5, 1% Triton X-100, 0.5% Nonidet P-40, 1 mM EDTA, 150 mM NaCl, 5 mM sodium pyrophosphate, 10 mM *p*-nitrophenyl phosphate, 10 mM β-glycerophosphate, 50 mM sodium fluoride and 1 mM sodium orthovanadate) for 30 min on ice, followed by centrifugation at 15 000 *g* for 15 min. The Tie-2 protein was immunoprecipitated from the cell lysate using protein Glutathione Sepharose 4B gel beads (Amersham Biosciences, Picataway, NJ, USA) coated with anti-Tie-2 antibody. After electrophoresis under reducing conditions using a gradient gel polyacrylamide (Bio-Rad), the immunoprecipitated Tie-2 proteins were transblotted onto a nitrocellulose membrane. The membrane was incubated with either 1 μg/mL anti-Tie-2 antibody or anti-phosphotyrosine (PTyr) antibody in a blocking buffer for 1 h. The membrane was washed and incubated with horseradish peroxidase-conjugated IgG, then developed as described above. The relative densities of the bands were measured using NIH image software (National Institutes of Health).

### Data analysis

Unless otherwise indicated, all data represent the mean ± SEM. An unpaired, two-tailed Student's *t*-test was used to determine the significance of differences between two groups means. One-way ANOVA followed by the modified Fisher's least-squares difference method was used to assess statistical significance of differences among means of more than two groups.

## Results

### Induction of occludin expression in TR-BBB13 cells by transfilter co-culture with TR-AST4 cells

The effect of transfilter co-culture with TR-AST4 cells on the expression levels of occludin and JAM was examined in TR-BBB13 cells (Fig. 1). The cells were co-cultured for 6 and 8 days, since it has been reported that cell-to-cell contact was observed between endothelial cells and astrocytes using the same transfilter pore size membrane for over 4 days (Hayashi *et al.* 1997). As shown in Fig. 1(a), the occludin mRNA levels in 6- and 8-day co-cultured TR-BBB13 cells were significantly increased compared with single culture (9.14- and 1.91-fold, respectively). In contrast, the JAM mRNA level was not changed significantly at either time point. To clarify whether occludin protein was increased